This is a preprint, the final version is subject to change, of the American Mineralogist (MSA)
Cite as Authors (Year) Title. American Mineralogist, in press.
DOI: http://dx.doi.org/10.2138/am-2018-6232

Revision 1

On the growth of witherite and its replacement by the Mg-bearing double carbonate norsethite – Implications for the dolomite problem

Michael Lindner* & Guntram Jordan

Department für Geo- und Umweltwissenschaften, Ludwig-Maximilians-Universität München, Theresienstr. 41, 80333 München, Germany.

** Corresponding author e-mail: michael.lindner@lrz.uni-muenchen.de*

Abstract

Witherite [$BaCO_3$] and norsethite [$BaMg(CO_3)_2$] are perceived as chemical and structural analogs of aragonite [$CaCO_3$] and dolomite [$CaMg(CO_3)_2$], respectively. However, norsethite, unlike dolomite, readily precipitates from aqueous solutions at ambient conditions. This is of special interest as the dehydration barrier of Mg^{2+} may be a likely cause of the dolomite growth inhibition. The easiness of norsethite growth shows that the problem of dolomite formation is more complex. In order to attain a comprehensive understanding of the analog $BaCO_3$-$MgCO_3$ system and of the formation of ordered anhydrous Mg-bearing double carbonates, we investigated the fate and behavior of aqueous magnesium during growth of witherite.

Growth experiments were conducted on witherite seeds in mixed-flow reactors at 50 °C and various Mg-concentrations (0.25-2 mM Ba^{2+}, 0-20 mM Mg^{2+}, pH 7.8-8.5, ionic strength 0.1 M). At Mg:Ba ratios in solution smaller than 6:1, Mg^{2+} did not affect witherite growth kinetics. No

significant amount of Mg^{2+} was incorporated. The rate constant k and reaction order n for witherite growth were determined for the first time ($k = 0.65 \pm 0.05 \cdot 10^{-7}$ mol m^{-2} s^{-1}; $n = 1.3 \pm 0.1$; supersaturation $\Omega = \frac{IAP}{K_s}$ = 1-4, where IAP is the ionic activity product and K_s the solubility constant). The insensitivity of witherite growth kinetics to these levels of Mg is analogous to aragonite growth. The general absence of the formation of solid solutions in the entire $BaCO_3$-$MgCO_3$ system, however, is not shared by the $CaCO_3$-$MgCO_3$ system, for which it is well known that substitution in the 6-fold coordinated cation sites occurs extensively.

Mg:Ba ratios in solution larger than 12:1 led to a replacement of witherite by norsethite. This replacement also is in strong contrast to the $CaCO_3$-$MgCO_3$ system, where higher temperatures and/or much longer timescales are necessary to obtain dolomite. The replacement rate of witherite at 50 °C was estimated to be ~200 times faster than the analogous replacement of aragonite by dolomite observed over 7 years at even 60 °C (Usdowski 1989).

We speculate that the preferential formation of ordered norsethite over a solid solution is facilitated by the large difference in Mg^{2+} and Ba^{2+} ionic radii. Due to the presumably very high free energy of formation of the solid solution, ordering into distinct Ba- and Mg-layers is the only way to combine both cations within one phase. In the $CaCO_3$-$MgCO_3$ system, solid solution occurrence is common and effectively contributes to the inhibition of the formation of the ordered double carbonate dolomite over a wide range of conditions (cf. Arvidson and Mackenzie 1999).

Keywords: carbonate growth kinetics, trace element incorporation, norsethite, barium mobility

Introduction

Witherite ($BaCO_3$) and norsethite [$BaMg(CO_3)_2$] (Mrose et al. 1961) have attracted much attention (Böttcher et al. 1997a, 1997b; Bucca et al. 2009; Busenberg and Plummer 1986b; De Villiers 1971; Franke et al. 1984; Hood et al. 1974; Königsberger et al. 1998; Lippmann 1968; Mavromatis et al. 2016; Pimentel and Pina 2014; Sánchez-Pastor et al. 2011; von Allmen et al. 2010) because these two minerals can be seen as analogous to aragonite ($CaCO_3$) and dolomite [$CaMg(CO_3)_2$] in the $CaCO_3$-$MgCO_3$ system. The concept of analogy is based on striking structural and chemical similarities. Witherite and aragonite are isostructural (De Villiers 1971). Dolomite and norsethite structures, in a simplified view, can be derived from the calcite structure where alternating Ca- and carbonate-layers lie perpendicular to the c-axis and every Ca^{2+} is coordinated by six equidistant oxygen ions (Lippmann 1973). In dolomite, every other Ca-layer is replaced by a Mg-layer. This replacement is accompanied by a small rotation of the carbonate groups resulting in smaller Mg-O and larger Ca-O distances. The resulting symmetry is reduced from $R\bar{3}c$ to $R\bar{3}$ (Lippmann 1973). Norsethite can be derived from dolomite by exchanging Ca with Ba, which causes a further rotation of the carbonate groups resulting in the space group $R\bar{3}c$ (Effenberger et al. 2014). Due to this carbonate rotation, Ba is irregularly and asymmetrically coordinated by six strongly bonded oxygens (like Ca in dolomite) and by six weakly bonded oxygens with a larger Ba-O distance (Ende et al. 2017). However, there is a far more important difference between norsethite and dolomite. Norsethite, unlike dolomite, readily grows from aqueous solutions at ambient temperatures within few days (Arvidson and Mackenzie 1999; Hood et al. 1974; Kaczmarek et al. 2014; Lippmann 1968; Rodriguez-Blanco et al. 2015). This discrepancy is of special interest as the dehydration barrier of Mg^{2+} was suggested to be the likely cause of the growth inhibition of dolomite (and magnesite) at low temperature (Hänchen et al. 2008; Lippmann 1973; Pokrovsky and Schott 2002). Dehydration of Mg^{2+}, however, is equally

part of both norsethite and dolomite growth. The relative ease with which norsethite can overcome this barrier shows that the problem of dolomite formation is more complex. Norsethite has been synthesized successfully by both a direct precipitation from Ba^{2+}-Mg^{2+}-CO_3^{2-} solutions and a reaction of witherite with Mg-containing water (Hood et al. 1974; Lippmann 1968). The detailed mechanism of dolomite formation, in contrast, is still under debate (e.g. Arvidson and Mackenzie 1999; Berninger et al. 2017; de Leeuw and Parker 2001; Fenter et al. 2007; Gregg et al. 2015; Higgins and Hu 2005; Kenward et al. 2013; Machel 2004; Rodriguez-Blanco et al. 2015; Yang et al. 2012; Zhang et al. 2012).

A further difference between the $CaCO_3$-$MgCO_3$ and the $BaCO_3$-$MgCO_3$ system is the polymorphism of $CaCO_3$. Unlike the $BaCO_3$-$MgCO_3$ system, the endmembers of the $CaCO_3$-$MgCO_3$ system can be structurally related or diverse. Consequently, $Ca_xMg_{1-x}CO_3$ solid solutions with calcite structure occur commonly, while aragonite does not incorporate significant amounts of magnesium (Berner 1975; Berninger et al. 2016; Mucci and Morse 1983). Furthermore, aqueous Mg has an inhibiting effect on the calcite growth rate, while aragonite growth is left unaffected (Astilleros et al. 2010; Berner 1975; Choudens-Sánchez and Gonzalez 2009; Davis et al. 2000; Wasylenki et al. 2005).

In isostructural carbonates, solid solution occurrence is generally related to cation radius differences (effective ionic radii, coordination number IV: Mg^{2+} = 0.72 Å, Ca^{2+} = 1.00 Å, Sr^{2+} = 1.18 Å, Ba^{2+} = 1.35 Å; Shannon 1976). A difference ≤ 0.11 Å usually leads to complete solid solutions, while larger differences may lead to solid solutions with limited miscibility (Reeder 1983). Following this argumentation in the $BaCO_3$-$MgCO_3$ system, no solid solution should be expected due to the large difference of cation radii ($r[Ba^{2+}]$ - $r[Mg^{2+}]$ = 0.63 Å). In fact, investigations of the growth of the Mg-rich endmember of the $BaCO_3$-$MgCO_3$ system revealed

that Ba is not incorporated into magnesite in significant amounts but norsethite is formed (Lindner et al. 2017); a similar behavior might be expected for the Mg-incorporation into witherite.

So far, studies of growth of witherite and its solid solutions (e.g. with $SrCO_3$) were mostly aimed at isotopic fractionation during mineral growth (Mavromatis et al. 2016; Prieto et al. 1997; Sánchez-Pastor et al. 2011). The growth of witherite under the influence of magnesium has not been investigated so far, although this system offers a unique opportunity to shed light on the behavior of aqueous magnesium during carbonate growth and the formation of an ordered anhydrous Mg-bearing double carbonate, which is directly related to the dolomite problem.

In order to attain a comprehensive understanding of the processes taking place during witherite growth and transformation to norsethite, this study aims to answer several questions: What is the rate constant of witherite growth i.e., what is the growth rate of witherite from solutions covering a significant span of different supersaturations. Does aqueous magnesium have an impact on witherite growth rates? Is magnesium incorporated into witherite during growth? Is norsethite precipitating from the Mg-bearing growth solutions? If yes, at which conditions? Answers to these questions, may considerably help to improve the understanding of why some anhydrous Mg-bearing carbonate minerals have severe growth problems but others not.

Materials and methods

Seed material and aqueous solutions

Natural witherite crystals (Settlingstones Mine, England) were used as seeds for all experiments. The crystals were crushed in an agate mortar and passed through stainless steel sieves. The size fraction 63-200 μm was used in all experiments. The crystals were washed several times with

deionized water and ethanol in an ultrasonic bath to remove particles and dried for several hours at 60 °C in an oven. The resulting powder consisted of crystal fragments without any identifiable crystal faces (Fig. 1a). As determined from SEM images, the average crystal diameter was 70 µm. Employing a cubic shape model, a specific surface area of 0.02 m^2/g was calculated. Solutions containing the desired concentrations of Ba and Mg cations and of CO_3 anions were prepared separately. The solutions were made by dissolving the respective solid chemicals ($BaCl_2 \cdot 2H_2O$, $MgCl_2 \cdot 6H_2O$, NaCl, $NaHCO_3$, Na_2CO_3, all p.a.) in deionized water with a resistivity of 18.2 MΩ cm. All solutions were adjusted to an ionic strength of 0.1 M using NaCl.

Mixed flow reactor setup and protocol

Growth experiments were performed in self-constructed PTFE mixed-flow reactors with a volume of approx. 200 ml (Fig. 2). Inlet and outlet of the reactor were equipped with nylon net filters with a pore size of 30 µm (Merck) to prevent loss of seed material. Furthermore, an externally driven magnetic stirring bar was placed inside the reactor in order to avoid sedimentation of the seed crystals and to ensure homogenous solution composition within the entire reactor. To maintain a constant temperature throughout the experiments (50 ± 1 °C), the reactors were submerged in a thermostatic water bath.

In order to avoid premature crystallization of carbonate phases in storage containers and tubing, both carbonate and Ba-Mg containing solutions were simultaneously pumped into the reactor from two separate collapsible PE containers using a two-channel peristaltic pump (GILSON Minipuls 3; Fig. 2). The flowrates of the two feed-lines were adjusted to be the same before the start of the experiment. During the experiments, the pump rates in the individual feed-lines were checked periodically by measuring the weight loss of the storage containers. The ratio of the two

feed rates did not vary significantly during an experiment and the total feed rate agreed well with the measured amount of effluent of the reactor. The starting conditions of the experiments are listed in table 1. Growth of crystals inside the reactor caused the solute concentration to decrease. This decrease ΔM could be measured by the difference between inlet and outlet solution concentration ($\Delta M = M^{in} - M^{out}$). The crystal growth rate R was then calculated by

$$R = \Delta M \, F / m \, S \qquad (1)$$

where F is the outlet flowrate, m is the initial mass of seed crystals and S is the specific surface area of the seed crystals.

After the concentration of the outflow had reached a constant value, crystal growth kinetics was assumed to be in steady state. Subsequently, flowrate was changed leading to a new steady state with a different solution composition within the reactor. After three or more different steady states had been established, the experimental run was finished and the reactor was opened. The crystals were retrieved by vacuum filtration using filter paper (Macherey-Nagel), quickly rinsed with deionized water and ethanol, and dried for at least 12 hours at 60 °C.

Analyses

Seed crystal powders were analyzed before and after the experiments by X-ray diffraction (GE Seifert, Cu $K_{\alpha 1}$ radiation; witherite PDF: 45-1471, norsethite PDF: 12-530) and SEM (Zeiss DSM 960 A). Solution pH and temperature was constantly monitored inside the reactor using an in-situ pH electrode (Meinsberger Elektroden EGA142), which was calibrated at the experimental temperature with pH 4.01, 7.01 and 10.01 buffers (Hanna Instruments). The outflow was collected periodically and the pH of the sample solution was measured immediately after cooling down to room temperature using a SI Instruments Titroline 7000 pH electrode A192, previously

calibrated with pH 4.01, 7.01 and 10.01 buffers (Hanna Instruments). Total alkalinity was determined by potentiometric end point titration with 0.01 M HCl with an uncertainty of ± 1 % and a detection limit of 2 x 10^{-5} eq/l (SI Instruments Titroline 7000, pH electrode A192). Ba^{2+} and Mg^{2+} concentrations were determined by potentiometric titration with 0.01 or 0.001 M Na_2-EDTA solutions with an uncertainty of ± 1 % and a detection limit of 2 x 10^{-5} molal (SI Instruments Titroline 7000, Ca ion selective electrode Ca1100, reference electrode B2920+).

The geochemistry program PhreeqC v. 3 (Parkhurst and Appelo) was used to model solution compositions, speciations and supersaturations. For the calculations, the llnl-database (Lawrence Livermore National Laboratory) had been modified by inserting the solubility constants of witherite ($\log_{10} K_{s\,wit}$= -8.562, Busenberg and Plummer 1986b), norsethite ($\log_{10} K_{s\,nrs}$= -16.72, Königsberger et al. 1998 - only 25 °C data available) and northupite ($Na_3Mg(CO_3)_2Cl$; $\log_{10} K_{s\,nrt}$= -4.8, Vančina et al. 1986). Mg^{2+} hydrolysis and carbonic acid dissociation equilibrium constants were modified after the values of Brown et al. (1996) and Millero et al. (2007), respectively. Furthermore, aqueous barium carbonate species ($BaHCO_3^+{}_{(aq)}$ and $BaCO_{3(aq)}$) and their stability constants (Busenberg and Plummer 1986b) were added to the database.

Results

Analyses of retrieved crystals

XRD patterns (Fig. 3) of product crystals retrieved from experiments with solutions with Mg:Ba concentration ratios ≤ 6:1 showed no other phase than witherite. The diffraction pattern of the crystals of the experiment with a Mg:Ba solution concentration ratio > 12:1, however, revealed a

mixture of witherite and norsethite. Rietveld refinement of the diffractogram yielded 90 wt% norsethite and 10 wt% witherite. Within the reactor, crystallization of different phases may have taken place to a different extent at different locations. Because the product crystals could not be retrieved from the reactor completely, XRD samples may not be entirely representative for the mineral assemblage inside the reactor. The composition determined by XRD, therefore, should be considered as a rough estimate.

SEM images of the retrieved crystals of experimental runs with Mg:Ba ≤ 6:1 revealed no significant change of morphology in comparison to the seed crystals. The product consisted of grown witherite seeds (Fig. 1b-d). However, crystals from the experiment with Mg:Ba > 12:1 mainly consisted of columns with lengths up to 70 μm, showing the same morphology as synthetic norsethite (e.g. Lipmann 1973). These crystals were partially covered by smaller crystallites with sizes of 0.2 to 2 μm, which can also be identified as norsethite (Fig. 1e & f). Only a small amount of the witherite seed material was recognizable, matching the large norsethite/witherite ratio determined by Rietveld analysis. Growth of the norsethite crystals on the witherite surfaces revealed no crystallographically preferred orientation. It should be noted that a decrease of seed crystal mass was detected only in the experiment where norsethite was found in the reactor (table 1). In other experimental runs, the mass of witherite increased.

Analyses of solutions

Solute concentrations of the effluent were measured in frequent intervals (table A1). From the individual samples, mean concentrations were calculated for each steady state condition (table 2). A significant decrease of input solution Mg besides total alkalinity and barium by the growth within the reactor was only detected in the experiment for which the X-ray diffractograms and SEM images revealed the formation of norsethite. The analyses of all other experiments revealed

a decrease of total alkalinities and barium but not of Mg in solution. From the latter experiments, witherite growth rates were calculated according to equation 1 based on the analyzed Ba decrease ($\Delta M = \Delta Ba$).

Witherite growth rates vs. solution supersaturation with respect to witherite showed no dependence on aqueous magnesium concentrations at Mg:Ba ≤ 6:1 (Fig.4). However, even at low supersaturations ($1<\Omega<3$), heterogeneous nucleation of witherite at the reactor walls, on the membranes and in the effluent tubing was evident. The precipitates led to an increased reactive surface area. In the calculation of the growth rates, the increase of the surface area has been taken into account by linearly increasing the mass of the crystals within the reactor with time while the specific surface area was kept constant. The total increase of mass was calculated on basis of the accumulated decrease of solutes from the inflow. Irrespective of the correction applied to the rate calculations, SEM images of retrieved crystals showed clearly that growth of the seed crystals rather than the newly nucleated crystals was the main cause of mass increase.

In the experimental run with Mg:Ba ratio > 12:1, witherite seed crystals dissolved and norsethite precipitated. The reactor solution of this experiment was obviously undersaturated with respect to witherite and supersaturated versus norsethite, as confirmed by PHREEQC calculations from the analyzed effluent concentrations.

Discussion

The growth rate of witherite

The conducted growth experiments represent the first systematic quantitative study of witherite growth kinetics covering a significant span of different solution supersaturations and additive concentrations. The results confirm the rough order of magnitude of growth rates of Mavromatis

et al. (2016) obtained from Mg-free solutions (Fig. 4). Due to the different temperature, though, one might expect that the data of Mavromatis et al. (2016) lie below the data obtained here throughout the entire range of conditions. Differences in solution speciation (e.g., Ba^{2+}/CO_3^{2-} ratio), experimental methodology (e.g., determination of specific surface area), and seed crystals may be accountable for these deviations. Measured growth rates $\boldsymbol{R}$ were fitted by the empirical equation

$$\boldsymbol{R = k(\Omega - 1)^n} \quad (2)$$

which is commonly used to calculate the rate constant $\boldsymbol{k}$ and the order $\boldsymbol{n}$ the growth reaction of experimental carbonate precipitation data (e.g. Arvidson and Mackenzie 1999; Berninger et al. 2016; Busenberg and Plummer 1986a; Gautier et al. 2015; Mucci and Morse 1983; Nancollas and Reddy 1971; Saldi et al. 2009). Our experiments yielded a rate constant $\boldsymbol{k}$ of $0.65 \pm 0.05 \cdot 10^{-7}$ mol m^{-2} s^{-1} and a reaction order $\boldsymbol{n}$ of 1.3 ± 0.1. A Mg:Ba ratio in solution of up to 6:1 had no discernible influence on measured witherite growth rates (Fig. 4).

The insignificance of incorporation of Mg into witherite

Based on the balance of the inflowing and outflowing solutions there was no reduction of Mg detectable within analytical limits (mean $\Delta Mg = 0.02 \pm 0.05$ mM), which implies that there is no incorporation of Mg into the growing witherite. This finding is in accordance with analyses of natural witherites (Pi et al. 2014), which showed Mg-concentrations of up to ≈ 0.12 wt%. Moreover, these low magnesium values may not even originate from incorporation into the witherite lattice exclusively but from a different accessory phase as well. The large difference in ionic radii of Ba and Mg (as illustrated by the fact that $MgCO_3$ precipitates in calcite structure

and $BaCO_3$ in aragonite structure) renders the incorporation of magnesium on Ba-sites unfavorable.

It is worth to compare the incorporation of Mg into witherite with the incorporation into aragonite. Based on linear free energy correlation, Wang and Xu (2001) predicted a partitioning of Mg between aragonite and solution at ambient conditions $\boldsymbol{log\ K_{d\ Mg\ Ara}} = \left(\frac{X_{Mg}}{X_{Ca}}\right)/\left(\frac{m_{Mg}}{m_{Ca}}\right) = \mathbf{-2.06}$ ($\boldsymbol{X_i}$: mole fraction of Ca^{2+} and Mg^{2+} in the precipitated aragonite, $\boldsymbol{m_i}$: concentration of Ca^{2+} and Mg^{2+} in aqueous solution). Dietzel et al. (2004) suggested that experimentally measured Mg incorporation during aragonite growth might likely be caused by complex adsorption and entrapment rather than by lattice site substitution. Ab-initio calculations suggested that Mg incorporation into aragonite is energetically reasonable, although the investigated range of substituent concentration (13-100 % Mg) is not observed in natural aragonites (Menadakis et al. 2009).

As the ionic radius of barium is much larger than that of calcium (1.35 Å vs. 1.00 Å) and the lattice mismatch, therefore, is much higher, the partition coefficient of Mg for witherite can be expected to be even lower than for aragonite. For trace elements with partition coefficients $K_d < 1$, the coefficients measured during crystal growth are likely higher than the equilibrium values (Rimstidt et al. 1998). Therefore, the lack of measurable incorporation of Mg into the growing witherite points to an extremely small equilibrium partition coefficient $K_{d\ Mg\ Wit} << 10^{-2}$. This result is in accordance with the findings in the inverse system, i.e., the very low incorporation of Ba into magnesite during growth (Lindner et al. 2017). This agreement supports the idea of a general absence of solid solution formation in the entire $BaCO_3$-$MgCO_3$ system.

The formation of norsethite

A Mg:Ba ratio > 12:1 in the growth solution led to witherite dissolution and norsethite precipitation (experiment WITMg 8). The ratio of barium and magnesium decreases in the solutions was in the range of $\Delta Ba:\Delta Mg \approx 1:2$ and did not correspond to the stoichiometry of $BaMg(CO_3)_2$. However, $(\Delta Ba+\Delta Mg):\Delta$alkalinity was about 1:2 in all samples, which implies a growth reaction according,

$$\mathbf{(Ba^{2+}, Mg^{2+})_2 + 4\,HCO_3^- \leftrightarrow (Ba, Mg)_2(CO_3)_2 + 2CO_2 + 2H_2O}$$

This equation is in good agreement for stoichiometric norsethite growth, if dissolution of witherite in the reactor provided the deficient amounts of Ba and CO_3^{2-}. Mass balance calculations of Ba and Mg decreases show that 4.2 mmoles Ba and 7 mmoles Mg were precipitated from the solution over the total experimental runtime of 10 days. The missing 2.8 mmoles Ba to form stoichiometric $BaMg(CO_3)_2$, therefore, may be assigned to dissolution of 0.55 g witherite seeds, yielding a composition of 17 % witherite and 83 % norsethite in the final product of the reactor. This result is supported by XRD and SEM analysis of the retrieved crystals, which showed norsethite to be the major component (~90 mass %). The assumption is further backed by the geochemical calculations of the solution speciation, which showed that the solutions were undersaturated with respect to witherite and strongly supersaturated with respect to norsethite.

Assuming that no Mg-bearing phase other than norsethite has been crystallizing (as evident from XRD and SEM), the Mg precipitation rate is equal to the norsethite growth rate. Norsethite growth rates, therefore, were calculated according to Eqn. (1) with $\Delta M = \Delta\, Mg^{2+}$ (table 3). The final surface area of norsethite was estimated from SEM images of the product powder employing a rectangular shape model with an average crystal size of 25x7x7 µm. The resulting specific surface area was 0.17 ± 0.07 m^2/g. Furthermore, it has been assumed that norsethite

surface area and mass increased linearly over experimental time starting from zero. Solution saturation states were calculated using the solubility product of norsethite at 50 °C ($\log K_{s\ nrs}^{50\ °C} = -17.57$), which has been obtained by linear interpolation of the $\log K_s$ vs. 1/T line given by the room temperature value from Königsberger et al. (1998) and the 100 °C value estimated by Lindner et al. (2017). The plot of growth rates against supersaturation reveals a positive correlation (Fig. 5). The fit of the data with Eqn. (2) yields a rate constant of $\boldsymbol{k} = 0.0020 \pm 0.0004 \cdot 10^{-7}$ mol m^{-2} s^{-1} and a reaction order of $\boldsymbol{n} = 2.0 \pm 0.1$. The comparison with norsethite growth rates at 100 °C (Lindner et al. 2017) confirms the expected positive correlation of the rate constant with temperature (Fig. 5).

The dissolution of witherite and precipitation of norsethite is in accordance with the synthesis experiments of Lippmann (1968, 1973), who immersed witherite in solutions with high magnesium concentrations (20 mM Mg^{2+}) at ambient conditions. From the solution, norsethite crystallized within days to weeks. In these experiments, dissolving witherite was the only Ba source. The Mg:Ba ratios of the solutions, therefore, were likely well above 12:1. In the mixed-flow reactor experiment conducted here, witherite in the reactor was not the only Ba source but aqueous Ba was constantly supplied by the feed solution. However, decrease of Ba by norsethite growth deprived the reactor in barium even below the solubility product of witherite. As long as solid $BaCO_3$ was present, dissolution of witherite tried to maintain the aqueous Ba concentration given by the solubility product of witherite. As no sign of epitaxial growth or passivation of the parental witherite crystals was detected in the SEM images, replacement of witherite by norsethite will continue until witherite is completely consumed. The witherite-norsethite replacement, therefore, can be classified as a dissolution-precipitation reaction (e.g. Putnis 2009) without any pseudomorphism of the newly formed phase being evident.

Comparison with the effect of Mg on $CaCO_3$ growth

Berner (1975) showed that magnesium slows calcite growth in artificial seawater but leaves aragonite growth rates unaffected. He concluded that Mg is not easily adsorbed on the aragonite surface or incorporated into the growing crystal and, thus, there is no effect on aragonite growth. This hypothesis was confirmed by Auger-spectroscopic measurements on the surface of aragonite following contact with seawater (Mucci and Morse 1985). As described above, Mg incorporation into aragonite is limited by a very small partition coefficient; for witherite, we observed a similar or even smaller partition coefficient. Our results further show that the growth rates of witherite are as unaffected by the presence of magnesium as the growth rates of the isostructural mineral aragonite (Berner 1975). Although the size difference between Ba^{2+} and Mg^{2+} is larger than between Ca^{2+} and Mg^{2+}, the structural and chemical similarities between aragonite and witherite suffice to facilitate the same insensitivity of growth rates to the presence of Mg^{2+} in amounts as studied here. Notable differences, however, occur in the presence of higher Mg concentrations common in lagoonal settings forming recent unordered Ca-Mg carbonates (e.g. Bathurst 1971; Lippmann 1973; Machel 2004; Usdowski 1967). At ambient conditions, witherite is rapidly replaced by the ordered double carbonate norsethite (e.g. Lippmann 1968) while parental $CaCO_3$ is left unaffected and a replacement by the ordered double carbonate dolomite has never been observed (Berner 1975; Choudens-Sánchez and Gonzalez 2009; Jonas et al. 2017; Land 1998; Usdowski 1989, 1994). Only at a temperature of 60 °C, Usdowski (1989, 1994) accomplished a replacement of 1 g aragonite in 7 years, while at the temperature of this study (50 °C) he still found both aragonite and calcite unaffected by the Mg-containing solution. Witherite, in contrast, dissolves at 50 °C (dissolved witherite/runtime: ~$2.6 \cdot 10^{-5}$ mol/h) and norsethite grows (total

precipitated norsethite/runtime: ~$3.0 \cdot 10^{-5}$ mol/h). This witherite-norsethite replacement at 50 °C is approx. 200 times faster than the replacement of aragonite by dolomite at 60 °C (Usdowski 1989, 1994).

The rapidity of norsethite growth in comparison to the sluggishness of dolomite formation is evident throughout the temperature range from ambient to 100 °C (Lindner et al. 2017; Lippmann 1968). This rate discrepancy clearly indicates that the slow ligand exchange of the Mg-aquo-complex cannot be the only factor inhibiting dolomite (and magnesite) precipitation at low temperatures. This finding is also supported by the failure to precipitate dolomite and magnesite from water-free solutions (Xu et al. 2013). Furthermore, the possibility to precipitate high-Mg calcite (Glover and Sippel 1967; Kitano and Kanamori 1966) and benstonite [$MgCa_6Ba_6(CO_3)_{13}$] (Hood and Steidl 1973) at room temperature within relatively short timescales clearly shows that the formation of unordered anhydrous carbonate minerals with moderate magnesium contents can be achieved easily. Moreover, the direct precipitation of ordered anhydrous Mg-bearing double carbonates from aqueous solution has been demonstrated at ambient conditions for norsethite (Böttcher et al. 1997b; Hood et al. 1974; Pimentel and Pina 2014) and $PbMg(CO_3)_2$ (Lippmann 1966; Morrow and Ricketts 1986; Pimentel and Pina 2016), but has not yet been achieved for dolomite at temperatures below 120 °C (e.g. Berninger et al. 2017; Land 1998; Higgins and Hu 2005).

Implications for the dolomite problem

As pointed out by Pimentel and Pina (2016), a structural component in the form of the different cation coordination polyhedra of Ca and Ba in dolomite and norsethite (and also of Pb in $PbMg(CO_3)_2$), respectively may have some influence on the ability to form an ordered double carbonate. Ca^{2+} can occur coordinated by six (calcite) and nine (aragonite) oxygen ions. Mg^{2+}

occupies sites with six-fold coordination exclusively. In dolomite, both Ca^{2+} and Mg^{2+} are coordinated by six oxygen ions. The similarity of coordination polyhedra of Ca^{2+} and Mg^{2+} is large enough to facilitate the mutual substitution of the two cations resulting in the precipitation of an unordered solid solution rather than of dolomite.

Ba^{2+} ions occur in nine-fold (witherite) and an irregular and asymmetric twelve-fold (norsethite) coordination (Ende et al. 2017, Effenberger et al. 2014; Lippmann 1973). In norsethite, therfore the coordination polyhedra of Ba^{2+} and Mg^{2+} are more different than the coordination polyhedra of Ca^{2+} and Mg^{2+} in dolomite. The difference in norsethite is large enough to preclude the substitution of cations by the high free energy of formation associated with BaO_6 and MgO_{12} polyhedra. Consequently, the formation of a $Ba_xMg_{1-x}CO_3$ solid solution is energetically unfavorable. In accordance with our experiments, the only way to combine both cations within one phase is ordering into distinct cation layers. The failure to form a solid solution, therefore, is an important prerequisite for the preferred occurrence of ordered norsethite. This preferential formation of norsethite is also in agreement with the findings of previous experiments at the Mg-rich boundary of the $BaCO_3$-$MgCO_3$ system (Lindner et al. 2017). Thus, it can be suggested that norsethite formation is favored not only at the Ba-rich boundary of the $BaCO_3$-$MgCO_3$ system but rather over the most part of the system.

The easiness of occurrence of the anhydrous ordered double carbonate in the $BaCO_3$-$MgCO_3$ system at low temperatures is in great contrast to the $CaCO_3$-$MgCO_3$ system. At temperatures below 60 °C, none of the different routes to form norsethite has been shown to exist for dolomite. All Mg:Ca ratios in solution fail to directly precipitate (ordered) dolomite. An unordered Ca-Mg-carbonate is strongly favored instead (e.g. Berninger et al. 2016; Mucci and Morse 1983). Adding Mg to calcite seeds leads to an unordered incorporation of Mg into the growing calcite (Mucci

and Morse 1983) and retards the growth rate. At the opposite boundary of the system, Ca is incorporated into growing magnesite seeds (without a noticeable effect on the growth rate; Berninger et al. 2016). The incorporation of the added ions into the growing seeds keeps the concentration of these ions in the growth solution low and counteracts nucleation of a new phase in the reactor. In other words, the formation of the Ca-Mg-carbonate solid solution is effectively inhibiting the precipitation of dolomite in experiments seeded with calcite or magnesite.

Acknowledgements

Support by the Deutsche Forschungsgemeinschaft DFG (JO301/4-1) is gratefully acknowledged. We thank Karin Paschert and Salvatore Carrocci for assistance with SEM and titration measurements, respectively. Furthermore, the authors are grateful for the two anonymous reviews and the editorial handling by Daniel Hummer.

REFERENCES CITED

Arvidson, R.S., and Mackenzie, F.T. (1999) The Dolomite Problem: Control of precipitation kinetics by temperature and saturation state. American Journal of Science, 299, 257–288 (en).

Astilleros, J.M., Fernández-Díaz, L., and Putnis, A. (2010) The role of magnesium in the growth of calcite: An AFM study. Chemical Geology, 271 (1-2), 52–58, DOI: 10.1016/j.chemgeo.2009.12.011 (en).

Bathurst, R.G.C. (1971) Carbonate sediments and their diagenesis, 620 p. Elsevier, Amsterdam (en).

Berner, R.A. (1975) The role of magnesium in the crystal growth of calcite and aragonite from sea water. Geochimica et Cosmochimica Acta, 39 (4), 489–504, DOI: 10.1016/0016-7037(75)90102-7 (en).

Berninger, U.-N., Jordan, G., Lindner, M., Reul, A., Schott, J., and Oelkers, E.H. (2016) On the effect of aqueous Ca on magnesite growth – Insight into trace element inhibition of carbonate mineral precipitation. Geochimica et Cosmochimica Acta, 178 (178), 195–209, DOI: 10.1016/j.gca.2016.01.019 (en).

Berninger, U.-N., Saldi, G.D., Jordan, G., Schott, J., and Oelkers, E.H. (2017) Assessing dolomite surface reactivity at temperatures from 40 to 120 °C by hydrothermal atomic force microscopy. Geochimica et Cosmochimica Acta, 199, 130–142, DOI: 10.1016/j.gca.2016.11.012 (en).

Böttcher, M.E., Gehlken, P.-L., Fernández-González, Á., and Prieto, M. (1997a) Characterization of synthetic $BaCO_3$ – $SrCO_3$ (witherite-strontianite) solid-solutions by Fourier transform infrared spectroscopy. European Journal of Mineralogy, 9 (3), 519–528, DOI: 10.1127/ejm/9/3/0519 (en).

Böttcher, M.E., Gehlken, P.-L., Skogby, H., and Reutel, C. (1997b) The vibrational spectra of $BaMg(CO_3)_2$ (norsethite). Mineralogical Magazine, 61, 249–256 (en).

Brown, P.L., Drummond, S.E., and Palmer, D.A. (1996) Hydrolysis of magnesium(II) at elevated temperatures. Journal of the Chemical Society, Dalton Transactions, 14, 3071, DOI: 10.1039/dt9960003071 (en).

Bucca, M., Dietzel, M., Tang, J., Leis, A., and Köhler, S.J. (2009) Nucleation and crystallization of otavite, witherite, calcite, strontianite, hydrozincite, and hydrocerussite by CO_2 membrane diffusion technique. Chemical Geology, 266 (3-4), 143–156, DOI: 10.1016/j.chemgeo.2009.06.002 (en).

Busenberg, E., and Plummer, L.N. (1986a) A Comparative Study of the Dissolution and Crystal Growth Kinetics of Calcite and Aragonite. In F.A. Mumpton, Ed., Studies in diagenesis, p. 139–168 (en).

Busenberg, E., and Plummer, L.N. (1986b) The solubility of $BaCO_3$(cr) (witherite) in CO_2-H_2O solutions between 0 and 90 °C, evaluation of the association constants of $BaHCO^{3+}$(aq) and $BaCO_3^0$(aq) between 5 and 80 °C, and a preliminary evaluation of the thermodynamic properties of Ba^{2+}(aq). Geochimica et Cosmochimica Acta, 50 (10), 2225–2233, DOI: 10.1016/0016-7037(86)90077-3 (en).

Choudens-Sánchez, V.D., and Gonzalez, L.A. (2009) Calcite and Aragonite Precipitation Under Controlled Instantaneous Supersaturation: Elucidating the Role of $CaCO_3$ Saturation State and Mg/Ca Ratio on Calcium Carbonate Polymorphism. Journal of Sedimentary Research, 79 (6), 363–376, DOI: 10.2110/jsr.2009.043 (en).

Davis, K.J., Dove, P.M., and De Yoreo, J.J. (2000) The Role of Mg^{2+} as an Impurity in Calcite Growth. Science (290), 1134–1137 (en).

de Leeuw, Nora H., and Parker, S.C. (2001) Surface–water interactions in the dolomite problem. Physical Chemistry Chemical Physics, 3 (15), 3217–3221, DOI: 10.1039/b102928m (en).

De Villiers, J.P. (1971) Cystal Structures of aragonite, strontianite and witherite. American Mineralogist, 56, 758–767 (en).

Dietzel, M., Gussone, N., and Eisenhauer, A. (2004) Co-precipitation of Sr^{2+} and Ba^{2+} with aragonite by membrane diffusion of CO_2 between 10 and 50 °C. Chemical Geology, 203 (1-2), 139–151, DOI: 10.1016/j.chemgeo.2003.09.008 (en).

Ende, M., Effenberger, H., and Miletich, R. (2017) Evolution of the α-$BaMg(CO_3)_2$ low-temperature superstructure and the tricritical nature of its α–β phase transition. Acta Crystallographica Section B Structural Science, Crystal Engineering and Materials, 73 (5), DOI: 10.1107/S2052520617009295.

Effenberger, H., Pippinger, T., Libowitzky, E., Lengauer, C.L., and Miletich, R. (2014) Synthetic norsethite, $BaMg(CO_3)_2$: revised crystal structure, thermal behaviour and displacive phase transition. Mineralogical Magazine, 78 (7), 1589–1611, DOI: 10.1180/minmag.2014.078.7.05 (en).

Fenter, P., Zhang, Z., Park, C., Sturchio, N.C., Hu, X.M., and Higgins, S.R. (2007) Structure and reactivity of the dolomite (104)–water interface: New insights into the dolomite problem. Geochimica et Cosmochimica Acta, 71 (3), 566–579, DOI: 10.1016/j.gca.2006.10.006 (en).

Franke, W., Hofer, A., Jelinski, B., and Lenk, K. (1984) The morphology of witherite and strontianite grown in Silica Gel, by slow precipitation and on hydrothermal conditions. Crystal Research and Technology, 19 (12), 1565–1569, DOI: 10.1002/crat.2170191209 (en).

Gautier, Q., Berninger, U.-N., Schott, J., and Jordan, G. (2015) Influence of organic ligands on magnesite growth: A hydrothermal atomic force microscopy study. Geochimica et Cosmochimica Acta, 155, 68–85, DOI: 10.1016/j.gca.2015.01.017 (en).

Glover, E.D., and Sippel, R.F. (1967) Synthesis of magnesium calcites. Geochimica et Cosmochimica Acta, 31 (4), 603–613, DOI: 10.1016/0016-7037(67)90037-3 (en).

Gregg, J.M., Bish, D.L., Kaczmarek, S.E., Machel, H.G., and Hollis, C. (2015) Mineralogy, nucleation and growth of dolomite in the laboratory and sedimentary environment: A review. Sedimentology, 62 (6), 1749–1769, DOI: 10.1111/sed.12202 (en).

Hänchen, M., Prigiobbe, V., Baciocchi, R., and Mazzotti, M. (2008) Precipitation in the Mg-carbonate system—effects of temperature and CO_2 pressure. Chemical Engineering Science, 63 (4), 1012–1028, DOI: 10.1016/j.ces.2007.09.052 (en).

Higgins, S.R., and Hu, X. (2005) Self-limiting growth on dolomite: Experimental observations with in situ atomic force microscopy. Geochimica et Cosmochimica Acta, 69 (8), 2085–2094, DOI: 10.1016/j.gca.2004.10.010 (en).

Hood, W.C., and Steidl, P.F. (1973) Synthesis of Benstonite at Room Temperatur. American Mineralogist, 58, 347-342 (en).

Hood, W.C., Steidl, P.F., and Tschopp, D.G. (1974) Precipitation of Norsethite at Room Temperature. American Mineralogist, 59, 471–474 (en).

Jonas, L., Müller, T., Dohmen, R., Immenhauser, A., and Putlitz, B. (2017) Hydrothermal replacement of biogenic and abiogenic aragonite by Mg-carbonates - Relation between textural control on effective element fluxes and resulting carbonate phase. Geochimica et Cosmochimica Acta, 196, 289–306, DOI: 10.1016/j.gca.2016.09.034 (en).

Kaczmarek, S.E., Sibley, D.F., and Immenhauser, A. (2014) Direct physical evidence of dolomite recrystallization. Sedimentology, 61 (6), 1862–1882, DOI: 10.1111/sed.12119 (en).

Kenward, P.A., Fowle, D.A., Goldstein, R.H., Ueshima, M., González, L.A., and Roberts, J.A. (2013) Ordered low-temperature dolomite mediated by carboxyl-group density of microbial cell walls. AAPG Bulletin, 97 (11), 2113–2125, DOI: 10.1306/05171312168 (af).

Kitano, Y., and Kanamori, N. (1966) Synthesis of magnesian calcite at low temperatures and pressures. Geochemical Journal, 1 (1), 1–10, DOI: 10.2343/geochemj.1.1 (en).

Königsberger, E., Tran-Ho, L.-C., and Gamsjäger, H. (1998) Solid-Solute Phase Equilibria in aqueous Solutions X. Solubility Constant and Stability of Norsethite. Monatshefte für Chemie, 129, 1061–1066 (en).

Land, L.S. (1998) Failure to Precipitate Dolomite at 25 °C from Dilute Solution Despite 1000-Fold Oversaturation after 32 Years. Aquatic Geochemistry, 4 (3/4), 361–368, DOI: 10.1023/A:1009688315854 (en).

Lindner, M., Saldi, G.D., Jordan, G., and Schott, J. (2017) On the effect of aqueous barium on magnesite growth – A new route for the precipitation of the ordered anhydrous Mg-bearing double carbonate norsethite. Chemical Geology, 460, 93–105, DOI: 10.1016/j.chemgeo.2017.04.019 (en).

Lippmann, F. (1966) $PbMg(CO_3)_2$, ein neues rhomboedrisches Doppelcarbonat. Die Naturwissenschaften, 53 (24), 701, DOI: 10.1007/BF00602722 (de).

Lippmann, F. (1968) Syntheses of $BaMg(CO_3)_2$ (Norsethite) at 20 °C and the Formation of Dolomite in Sediments. In G. Müller and G.M. Friedman, Eds., Recent Developments in Carbonate Sedimentology in Central Europe, p. 33–37. Springer, Berlin, Heidelberg (en).

Lippmann, F. (1973) Sedimentary carbonate minerals, 228 p. Springer, Berlin (eng).

Machel, H.G. (2004) Concepts and models of dolomitization: A critical reappraisal. Geological Society, London, Special Publications, 235 (1), 7–63, DOI: 10.1144/GSL.SP.2004.235.01.02 (en).

Mavromatis, V., van Zuilen, K., Purgstaller, B., Baldermann, A., Nägler, T.F., and Dietzel, M. (2016) Barium isotope fractionation during witherite ($BaCO_3$) dissolution, precipitation and at equilibrium. Geochimica et Cosmochimica Acta, 190, 72–84, DOI: 10.1016/j.gca.2016.06.024 (en).

Menadakis, M., Maroulis, G., and Koutsoukos, P.G. (2009) Incorporation of Mg^{2+}, Sr^{2+}, Ba^{2+} and Zn^{2+} into aragonite and comparison with calcite. Journal of Mathematical Chemistry, 46 (2), 484–491, DOI: 10.1007/s10910-008-9490-4 (en).

Millero, F.J., Huang, F., Graham, T., and Pierrot, D. (2007) The dissociation of carbonic acid in NaCl solutions as a function of concentration and temperature. Geochimica et Cosmochimica Acta, 71 (1), 46–55, DOI: 10.1016/j.gca.2006.08.041 (en).

Morrow, D.W., and Ricketts, B.D. (1986) Chemical controls on the precipitation of mineral analogues of dolomite: The sulfate enigma. Geology (14), 408–410 (en).

Morse, J.W., Wang, Q., and Tsio, M.Y. (1997) Influences of temperature and Mg:Ca ratio on $CaCO_3$ precipitates from seawater. Geology, 25 (1), 85, DOI: 10.1130/0091-7613(1997)025<0085:IOTAMC>2.3.CO;2 (en).

Mrose, M.E., Chao, E., Fahey, J.J., and Milton, C. (1961) Norsethite, $BaMg(CO_3)_2$, a new Mineral from the Green River Formation, Wyoming. American Mineralogist (46), 420–429 (en).

Mucci, A., and Morse, J.W. (1983) The incorporation of Mg^{2+} and Sr^{2+} into calcite overgrowths: influences of growth rate and solution composition. Geochimica et Cosmochimica Acta, 47 (2), 217–233, DOI: 10.1016/0016-7037(83)90135-7 (en).

Mucci, A., and Morse, J.W. (1985) Auger spectroscopy determination of the surface-most adsorbed layer composition on aragonite, calcite, dolomite, and magnesite in synthetic seawater. American Journal of Science, 285 (4), 306–317, DOI: 10.2475/ajs.285.4.306 (en).

Nancollas, G.H., and Reddy, M.M. (1971) The crystallization of calcium carbonate: II. Calcite growth mechanism. Journal of colloid and interface science, 37 (4), 824–830, DOI: 10.1016/0021-9797(71)90363-8 (en).

Parkhurst, D.L., and Appelo, C.A.J. Description of input and examples for PHREEQC version 3-A computer program for speciation, batch-reaction, one-dimensional transport, and inverse geochemical calculations, U.S. Geological Survey Techniques and Methods (en).

Pimentel, C., and Pina, C.M. (2014) The formation of the dolomite-analogue norsethite: Reaction pathway and cation ordering. Geochimica et Cosmochimica Acta, 142, 217–223, DOI: 10.1016/j.gca.2014.07.021 (en).

Pimentel, C., and Pina, C.M. (2016) Reaction pathways towards the formation of dolomite-analogues at ambient conditions. Geochimica et Cosmochimica Acta, 178, 259–267, DOI: 10.1016/j.gca.2015.12.040 (en).

Pokrovsky, O.S., and Schott, J. (2002) Surface Chemistry and Dissolution Kinetics of Divalent Metal Carbonates. Environmental Science & Technology, 36 (3), 426–432, DOI: 10.1021/es010925u (en).

Prieto, M., Fernández-González, A., Putnis, A., and Fernández-Díaz, L. (1997) Nucleation, growth, and zoning phenomena in crystallizing $(Ba,Sr)CO_3$, $Ba(SO_4,CrO_4)$, $(Ba,Sr)SO_4$, and $(Cd,Ca)CO_3$ solid solutions from aqueous solutions. Geochimica et Cosmochimica Acta, 61 (16), 3383–3397, DOI: 10.1016/S0016-7037(97)00160-9 (en).

Putnis, A. (2009) Mineral Replacement Reactions. Reviews in Mineralogy and Geochemistry, 70 (1), 87–124, DOI: 10.2138/rmg.2009.70.3.

Reeder, R.J. (1983) Crystal chemistry of the rhombohedral carbonates. In R.J. Reeder, Ed., Carbonates: Mineralogy and chemistry, 11, p. 1–47. Reviews in mineralogy, Mineralogical Soc. of America, Washington, D.C. (en).

Rimstidt, J., Balog, A., and Webb, J. (1998) Distribution of trace elements between carbonate minerals and aqueous solutions. Geochimica et Cosmochimica Acta, 62 (11), 1851–1863, DOI: 10.1016/S0016-7037(98)00125-2 (en).

Rodriguez-Blanco, J.D., Shaw, S., and Benning, L.G. (2015) A route for the direct crystallization of dolomite. American Mineralogist, 100 (5-6), 1172–1181, DOI: 10.2138/am-2015-4963 (en).

Saldi, G.D., Jordan, G., Schott, J., and Oelkers, E.H. (2009) Magnesite growth rates as a function of temperature and saturation state. Geochimica et Cosmochimica Acta, 73 (19), 5646–5657, DOI: 10.1016/j.gca.2009.06.035 (en).

Sánchez-Pastor, N., Gigler, A.M., Jordan, G., Schmahl, W.W., and Fernández-Díaz, L. (2011) Raman Study of Synthetic Witherite–Strontianite Solid Solutions. Spectroscopy Letters, 44 (7-8), 500–504, DOI: 10.1080/00387010.2011.610409 (en).

Shannon, R.D. (1976) Revised effective ionic radii and systematic studies of interatomic distances in halides and chalcogenides. Acta Crystallographica Section A, 32 (5), 751–767, DOI: 10.1107/S0567739476001551 (en).

Usdowski, H.-E. (1967) Die Genese von Dolomit in Sedimenten Springer-Verlag, Berlin (de).

Usdowski, H.-E. (1989) Synthesis of dolomite and magnesite at 60 °C in the system Ca-Mg-CO_3^{2-}-Cl_2-H_2O. Naturwissenschaften, 76, 374–375 (en).

Usdowski, E. (1994) Synthesis of Dolomite and Geochemical Implications. In B. Purser, M. Tucker, and D. Zenger, Eds., Dolomites: A Volume in Honour of Dolomieu, p. 345–360. Blackwell Publishing Ltd, Oxford (en).

Vančina, V., Plavšić, M., Bilinski, H., Branica, M., and Millero, F.J. (1986) Preparation and solubility of northupite from brine and its adsorption properties for Cu(II) and Cd(II) in seawater. Geochimica et Cosmochimica Acta, 50 (7), 1329–1336, DOI: 10.1016/0016-7037(86)90309-1 (en).

von Allmen, K., Böttcher, M.E., Samankassou, E., and Nägler, T.F. (2010) Barium isotope fractionation in the global barium cycle: First evidence from barium minerals and precipitation experiments. Chemical Geology, 277 (1-2), 70–77, DOI: 10.1016/j.chemgeo.2010.07.011 (en).

Wasylenki, L.E., Dove, P.M., and De Yoreo, J.J. (2005) Effects of temperature and transport conditions on calcite growth in the presence of Mg^{2+}: Implications for paleothermometry. Geochimica et Cosmochimica Acta, 69 (17), 4227–4236, DOI: 10.1016/j.gca.2005.04.006 (en).

Xu, J., Yan, C., Zhang, F., Konishi, H., Xu, H., and Teng, H.H. (2013) Testing the cation-hydration effect on the crystallization of Ca-Mg-CO_3 systems. Proceedings of the National Academy of Sciences of the United States of America, 110 (44), 17750–17755, DOI: 10.1073/pnas.1307612110 (en).

Yang, Y., Sahai, N., Romanek, C.S., and Chakraborty, S. (2012) A computational study of Mg^{2+} dehydration in aqueous solution in the presence of HS^- and other monovalent anions – Insights to dolomite formation. Geochimica et Cosmochimica Acta, 88, 77–87, DOI: 10.1016/j.gca.2012.03.018 (en).

Zhang, F., Xu, H., Konishi, H., Shelobolina, E.S., and Roden, E.E. (2012) Polysaccharide-catalyzed nucleation and growth of disordered dolomite: A potential precursor of sedimentary dolomite. American Mineralogist, 97 (4), 556–567, DOI: 10.2138/am.2012.3979 (en).

Figure captions

Figure 1. SEM images of crystals before (a) and after experiments without Mg (b), Mg:Ba ≤ 1:1 (c), and Mg:Ba ≤ 6:1 (d) show no difference to the used seed crystals. Mg:Ba > 12:1 (e & f) lead to dissolution of witherite and formation of many small norsethite needles.

Figure 2. Experimental set-up of mixed flow reactor with in-situ pH-electrode. The two input solutions are mixed inside the reactor to avoid supersaturation and precipitation in the absence of seed crystals. The PTFE reactor is placed inside a water bath for constant temperature.

Figure 3. X-ray diffractograms of seeds and retrieved crystals. All experiments with Mg:Ba ≤ 6:1 yielded only witherite (WIT), except for experiment WITMg 8 (Mg:Ba >12:1, top), which is mostly norsethite (NRS). Rietveld refinement yields a mixture of 90 wt% norsethite and 10 wt% witherite.

Figure 4. Witherite growth rate vs. supersaturation Ω with respect to witherite. Black symbols stand for Mg-containing samples with Mg:Ba ≤ 6:1, white symbols for Mg-free samples. There is no effect of Mg on the growth rates detectable. Data for norsethite precipitating experiment is not shown. Asterisks refer to values of Mavromatis et al. (2016). The line refers to a fit with the equation $R=k(\Omega-1)^n$ with $k = 0.65 \cdot 10^{-7}$ mol m^{-2} s^{-1} and $n = 1.3$

Figure 5. Norsethite growth rates vs. norsethite supersaturation. The first three samples give higher supersaturations and faster corresponding growth rates than the following samples. Rates are comparable to norsethite growth rates obtained at 100 °C (Lindner et al. 2017). The data has been fitted with an equation of the form $R=k(\Omega-1)^n$. For details on calculation method, see text.

This is a preprint, the final version is subject to change, of the American Mineralogist (MSA)
Cite as Authors (Year) Title. American Mineralogist, in press.
DOI: http://dx.doi.org/10.2138/am-2018-6232

Tables

Table 1. Starting conditions of the mixed-flow reactor experiments as well as masses of recovered crystals. Inlet solutions from containers 1 and 2 were pumped into the reactor with a ratio of 1:1. Resulting reactor Mg:Ba ratios and supersaturations Ω for norsethite and witherite are also given.

	Container 1				Container 2								
Experiment	Ba [mM]	Mg [mM]	NaCl [mM]	pH_{RT}	$NaHCO_3$ [mM]	NaCl [mM]	pH_{RT}	Mg:Ba	Ω witherite	Ω norsethite	crystals start [g]	crystals end [g]	Δ crystal mass [g]
WIT 6	3	-	97	5.64	10	90	8.35	-	4.0	-	1.225	2.218	0.993
WIT 7	0.5	-	97	5.47	25	80	8.30	-	1.9	-	1.005	1.539	0.534
WIT 8	2	-	95	5.55	20	90	8.46	-	5.8	-	1.505	4.13	2.625
WIT 11	2	-	95	5.60	20	90	8.30	-	5.8	-	1.497	2.402	0.905
WIT 12	2	-	90	5.69	10[a]	90	8.61	-	6.2	-	1.007	1.382	0.372
WITMg 7	0.5	0.05	97	5.52	25	80	8.28	0.1	1.9	0.9	1.005	1.532	0.527
WITMg 8	4	40	10	5.88	20	60	8.40	10	5.0	631.0	1.293	0.765	-0.528
WITMg 9	2	2	95	5.61	20	90	8.31	1	5.2	67.6	1.500	3.659	2.159
WITMg 10	4	4	78	5.55	11	90	8.21	1	5.1	67.6	1.501	2.105	0.604
WITMg 11	2	0.2	95	5.59	20	90	8.28	0.1	5.6	7.9	1.498	2.081	0.583
WITMg 12	2	6	90	5.63	10[a]	90	8.60	3	4.3	138.0	1.015	1.285	0.270

[a]additionally 0.25 mM Na_2CO_3 was added to the solution.

Table 2. Mean values of steady state conditions of the mixed-flow reactor experiments.

Sample	flowrate [ml/min]	pH [50°C]	total alkalinity [meq/l]	Ba^{2+} [mM]	Mg^{2+} [mM]	Mg:Ba	Δ total alkalinity [meq/l]	Δ Ba^{2+} [mM]	Δ Mg^{2+} [mM]	$Rate_{WIT}$ [10^{-7} mol m^{-2} s^{-1}]	Ω witherite
WIT 6 6-8	0.2	7.79	4.16	1.07	-	-	0.79	0.42	-	0.48 ± 0.05	1.9 ± 0.2
WIT 6 11-13	0.5	7.69	4.32	1.16	-	-	0.63	0.34	-	0.69 ± 0.07	1.7 ± 0.2
WIT 6 18-20	0.1	7.79	3.79	0.90	-	-	1.19	0.59	-	0.27 ± 0.03	1.5 ± 0.1
WIT 6 25-26	0.9	7.76	4.37	1.19	-	-	0.58	0.31	-	1.1 ± 0.1	2.1 ± 0.2
WIT 7 8-16	0.2	8.53	11.92	0.06	-	-	0.28	0.24	-	0.18 ± 0.02	1.5 ± 0.1
WIT 7 18-27	0.4	8.38	11.80	0.08	-	-	0.41	0.21	-	0.31 ± 0.03	1.6 ± 0.2
WIT 7 31-40	0.8	8.27	11.94	0.13	-	-	0.12	0.13	-	0.36 ± 0.04	1.9 ± 0.2
WIT 8 1-8	0.1	8.05	8.35	0.26	-	-	1.60	0.73	-	0.31 ± 0.03	1.6 ± 0.2
WIT 8 9-15	0.5	8.02	8.79	0.38	-	-	1.16	0.60	-	1.0 ± 0.1	2.3 ± 0.2
WIT 8 16-21	1.0	7.93	8.88	0.46	-	-	1.07	0.52	-	1.4 ± 0.1	2.4 ± 0.2

This is a preprint, the final version is subject to change, of the American Mineralogist (MSA)
Cite as Authors (Year) Title. American Mineralogist, in press.
DOI: http://dx.doi.org/10.2138/am-2018-6232

Sample	flowrate [ml/min]	pH [50°C]	total alkalinity [meq/l]	Ba^{2+} [mM]	Mg^{2+} [mM]	Mg:Ba	Δ total alkalinity [meq/l]	Δ Ba^{2+} [mM]	Δ Mg^{2+} [mM]	$Rate_{WIT}$ [10^{-7} mol m^{-2} s^{-1}]	Ω witherite
WIT 8 22-24	1.3	8.02	8.89	0.49	-	-	1.07	0.49	-	1.7 ± 0.2	3.1 ± 0.3
WIT 8 25-28	1.6	7.98	8.89	0.51	-	-	1.06	0.47	-	2 ± 0.2	2.9 ± 0.3
WIT 8 29-36	1.9	8.07	8.84	0.52	-	--	1.11	0.47	-	2.2 ± 0.2	3.6 ± 0.4
WIT 8 37-40	1.7	8.04	8.50	0.54	-	-	1.45	0.44	-	1.7 ± 0.2	3.4 ± 0.3
WIT 11 2-5	0.1	8.01	8.26	0.27	-	-	1.66	0.78	-	0.5 ± 0.05	1.5 ± 0.2
WIT 11 6-8	0.2	8.00	8.72	0.29	-	-	1.20	0.75	-	0.73 ± 0.07	1.7 ± 0.2
WIT 11 9-12	0.5	8.05	8.67	0.42	-	-	1.25	0.62	-	1.4 ± 0.1	2.8 ± 0.3
WIT 11 13-16	0.7	8.06	8.74	0.46	-	-	1.18	0.58	-	1.8 ± 0.2	3.1 ± 0.3
WIT 11 17-21	1.0	8.08	8.81	0.47	-	-	1.11	0.58	-	2.5 ± 0.3	3.3 ± 0.3
WIT 12 1-5	0.2	7.99	4.50	0.65	-	-	0.78	0.37	-	0.49 ± 0.05	2.0 ± 0.2
WIT 12 6-10	0.5	8.04	4.75	0.72	-	-	0.54	0.30	-	1.1 ± 0.1	2.6 ± 0.3
WIT 12 11-15	1.0	8.14	4.84	0.74	-	-	0.44	0.27	-	2 ± 0.2	3.4 ± 0.3
WIT 12 16-19	0.6	8.10	4.74	0.72	-	-	0.54	0.30	-	1.4 ± 0.1	2.9 ± 0.3
WITMg 7 1-10	0.2	8.59	11.64	0.04	0.03	0.8	0.64	0.25	0.00	0.21 ± 0.02	1.2 ± 0.1
WITMg 7 11-16	0.1	8.62	11.78	0.05	0.03	0.7	0.50	0.25	0.00	0.2 ± 0.02	1.3 ± 0.1
WITMg 7 18-29	0.4	8.49	11.72	0.07	0.03	0.5	0.54	0.21	0.00	0.37 ± 0.04	1.6 ± 0.2
WITMg 7 31-40	0.7	8.46	11.76	0.10	0.03	0.2	0.27	0.14	0.00	0.5 ± 0.05	2.2 ± 0.2
WITMg 8 10-19	0.4	7.03	7.17	1.39	17.20	12.3	2.78	0.64	2.95	-	0.7 ± 0.1
WITMg 8 22-25	0.6	7.03	7.48	1.45	19.42	13.4	2.47	0.58	0.72	-	0.7 ± 0.1
WITMg 8 29-32	1.1	7.06	7.70	1.57	19.46	12.4	2.24	0.47	0.69	-	0.8 ± 0.1
WITMg 9 1-8	0.1	7.98	8.68	0.17	0.99	5.9	1.52	0.81	0.01	0.42 ± 0.04	1.3 ± 0.1
WITMg 9 9-13	0.6	8.01	8.87	0.34	1.03	3.0	1.33	0.64	-0.03	1.1 ± 0.1	3.0 ± 0.3
WITMg 9 14-18	1.1	7.97	8.92	0.38	0.97	2.6	1.28	0.60	0.03	1.9 ± 0.2	3.0 ± 0.3
WITMg 9 19-22	0.4	8.06	8.79	0.25	0.98	3.9	1.41	0.72	0.02	0.74 ± 0.07	2.4 ± 0.2
WITMg 9 23-26	1.4	8.03	8.90	0.38	0.99	2.6	1.30	0.60	0.02	2.3 ± 0.2	3.5 ± 0.3
WITMg 9 27-30	0.1	8.05	8.45	0.16	0.97	6.1	1.75	0.82	0.03	0.27 ± 0.03	1.5 ± 0.1
WITMg 10 1-5	1.0	7.81	4.72	1.70	2.12	1.2	0.68	0.36	0.00	2 ± 0.2	3.4 ± 0.3
WITMg 10 6-10	1.9	7.83	4.79	1.75	2.03	1.2	0.61	0.31	0.09	3.2 ± 0.3	3.8 ± 0.4
WITMg 10 11-15	1.4	7.83	4.77	1.73	2.10	1.2	0.63	0.33	0.02	2.4 ± 0.2	3.7 ± 0.4
WITMg 10 16-18	0.2	7.83	3.89	1.21	2.14	1.8	1.51	0.85	-0.02	0.85 ± 0.09	2.1 ± 0.2
WITMg 11 1-5	0.1	7.93	7.42	0.29	0.09	0.3	2.38	0.78	0.01	0.48 ± 0.05	1.8 ± 0.2
WITMg 11 6-8	0.2	7.90	8.43	0.34	0.13	0.4	1.37	0.73	-0.03	0.76 ± 0.08	2.3 ± 0.2
WITMg 11 9-12	0.5	7.90	8.61	0.45	0.13	0.3	1.19	0.62	-0.03	1.3 ± 0.1	3.0 ± 0.3
WITMg 11 13-16	0.7	7.89	8.74	0.49	0.14	0.3	1.06	0.58	-0.04	1.6 ± 0.2	3.3 ± 0.3
WITMg 11 17-21	1.0	7.90	8.80	0.50	0.15	0.3	1.00	0.56	-0.05	2.2 ± 0.2	3.5 ± 0.3
WITMg 12 1-5	0.2	7.90	4.47	0.67	2.83	4.2	0.85	0.33	0.15	0.40 ± 0.05	1.5 ± 0.2
WITMg 12 6-10	0.5	7.89	4.76	0.78	2.93	3.7	0.56	0.21	0.05	0.71 ± 0.08	1.9 ± 0.2

This is a preprint, the final version is subject to change, of the American Mineralogist (MSA)
Cite as Authors (Year) Title. American Mineralogist, in press.
DOI: http://dx.doi.org/10.2138/am-2018-6232

Sample	flowrate [ml/min]	pH [50°C]	total alkalinity [meq/l]	Ba^{2+} [mM]	Mg^{2+} [mM]	Mg:Ba	Δ total alkalinity [meq/l]	Δ Ba^{2+} [mM]	Δ Mg^{2+} [mM]	$Rate_{WIT}$ [10^{-7} mol m^{-2} s^{-1}]	Ω witherite
WITMg 12 11-15	0.9	7.93	4.80	0.82	2.94	3.6	0.52	0.17	0.04	1.1 ± 0.1	2.2 ± 0.2
WITMg 12 16-19	0.6	7.93	4.74	0.80	2.90	3.6	0.58	0.20	0.08	0.79 ± 0.08	2.1 ± 0.2

Table 3. Effluent results of experiment WITMg 8, which precipitated norsethite. Cumulative amounts of precipitated barium and magnesium over the run of the experiment based on mass balance calculations of the wet chemical analyses are given. Norsethite growth rates ($Rate_{NRS}$) have been calculated using the decrease in solution Mg and a surface area estimated from SEM images of retrieved crystals.

Sample	Flowrate [ml/min]	pH [50 °C]	Mg:Ba	Δ Ba [mM]	Δ Mg [mM]	Δ alkalinity [meq/l]	Ω witherite	Ω norsethite	cum. Ba precip. [mmol]	cum. Mg precip. [mmol]	$Rate_{NRS}$ [10^{-7} mol m^{-2} s^{-1}]
WITMg 8-1	0.4	8.18	23.5	1.30	3.03	2.68	1.3	96.8	0.56	1.30	18 ± 5
WITMg 8-2	0.5	8.18	22.0	1.21	2.03	2.48	1.1	69.5	0.63	1.42	12 ± 3
WITMg 8-3	0.4	8.19	21.9	1.21	2.04	2.39	1.2	74.4	0.67	1.50	10 ± 3
WITMg 8-5	0.4	8.06	24.8	1.24	0.54	2.44	0.6	24.8	0.78	1.54	1.2 ± 0.3
WITMg 8-6	0.4	8.06	22.3	1.14	0.31	2.44	0.7	25.5	0.90	1.57	0.7 ± 0.2
WITMg 8-7	0.4	8.02	17.5	0.91	0.50	2.62	0.7	24.4	1.28	1.79	0.8 ± 0.2
WITMg 8-8	0.4	8.03	16.9	0.88	0.76	2.69	0.7	23.3	1.36	1.85	1.1 ± 0.3
WITMg 8-9	0.4	8.05	14.9	0.75	1.01	2.78	0.8	24.2	1.42	1.93	1.4 ± 0.4
WITMg 8-10	0.4	7.97	13.5	0.61	1.04	3.00	0.7	15.9	2.42	3.64	0.7 ± 0.2
WITMg 8-11	0.4	8.00	13.2	0.59	1.07	2.96	0.7	16.3	2.46	3.70	0.7 ± 0.2
WITMg 8-12	0.4	7.95	13.5	0.62	1.18	2.96	0.7	15.2	2.52	3.81	0.8 ± 0.2
WITMg 8-13	0.4	8.00	13.8	0.63	0.77	2.97	0.7	16.0	2.79	4.14	0.5 ± 0.1
WITMg 8-14	0.4	8.12	11.6	0.40	1.15	2.49	0.8	19.9	2.80	4.18	0.6 ± 0.2
WITMg 8-15	0.4	8.09	12.3	0.46	0.77	2.48	0.8	17.7	2.82	4.21	0.4 ± 0.1
WITMg 8-17	0.4	8.05	11.3	0.35	1.15	2.83	0.7	15.6	2.98	4.74	0.6 ± 0.2
WITMg 8-18	0.4	8.06	11.5	0.36	1.01	2.69	0.7	16.1	2.99	4.78	0.5 ± 0.1
WITMg 8-19	0.5	8.05	11.2	0.34	1.17	2.80	0.7	15.1	3.01	4.84	0.7 ± 0.2
WITMg 8-20	0.7	7.90	11.2	0.34	1.14	2.55	0.8	17.7	3.05	4.99	0.9 ± 0.2
WITMg 8-21	0.6	7.90	12.1	0.46	1.19	2.46	0.8	19.2	3.35	5.77	0.9 ± 0.2
WITMg 8-22	0.6	7.90	17.0	0.86	0.29	2.54	0.6	13.8	3.39	5.78	0.2 ± 0.1
WITMg 8-23	0.7	7.90	12.6	0.50	0.93	2.54	0.7	17.7	3.44	5.87	0.7 ± 0.2
WITMg 8-24	0.7	7.90	12.2	0.46	0.89	2.48	0.8	18.5	3.47	5.93	0.6 ± 0.2
WITMg 8-25	0.6	7.91	12.6	0.49	0.79	2.31	0.8	18.9	3.50	5.97	0.6 ± 0.1
WITMg 8-26	1.1	7.80	12.0	0.43	0.88	2.32	0.8	21.5	3.53	6.04	1.1 ± 0.3

This is a preprint, the final version is subject to change, of the American Mineralogist (MSA)
Cite as Authors (Year) Title. American Mineralogist, in press.
DOI: http://dx.doi.org/10.2138/am-2018-6232

Sample	Flowrate [ml/min]	pH [50 °C]	Mg:Ba	Δ Ba [mM]	Δ Mg [mM]	Δ alkalinity [meq/l]	Ω witherite	Ω norsethite	cum. Ba precip. [mmol]	cum. Mg precip. [mmol]	$Rate_{NRS}$ [10^{-7} mol m^{-2} s^{-1}]
WITMg 8-27	1.1	7.75	12.6	0.49	0.70	2.29	0.8	21.0	4.04	6.77	0.8 ± 0.2
WITMg 8-28	1.1	7.75	12.8	0.50	0.60	2.29	0.8	19.9	4.08	6.83	0.7 ± 0.2
WITMg 8-29	1.1	7.75	12.2	0.45	0.76	2.24	0.9	22.8	4.14	6.92	0.9 ± 0.2
WITMg 8-30	1.1	7.74	12.3	0.46	0.76	2.22	0.9	22.7	4.17	6.97	0.8 ± 0.2
WITMg 8-31	1.1	7.76	12.8	0.50	0.47	2.26	0.8	21.1	4.20	7.00	0.5 ± 0.1
WITMg 8-32	1.1	7.74	12.3	0.46	0.75	2.26	0.8	21.4	4.23	7.04	0.8 ± 0.2

Table A1. Results of single mixed-flow reactor samples.

Sample	flowrate [ml/min]	pH [50°C]	total alkalinity [meq/l]	Ba^{2+} [mM]	Mg^{2+} [mM]	Mg:Ba	Δ total alkalinity [meq/l]	Δ Ba^{2+} [mM]	Δ Mg^{2+} [mM]	Rate [10^{-7} mol/m^2s^{-1}]	Ω witherite	Ω norsethite
WIT 6-01	0.3	7.79	2.98	0.85	-	-	1.96	0.65	-	0.9	1.1	-
WIT 6-02	0.3	7.80	3.29	0.92	-	-	1.58	0.61	-	0.8	1.3	-
WIT 6-03	0.2	7.73	4.19	1.13	-	-	0.80	0.36	-	0.4	1.8	-
WIT 6-04	0.2	7.72	4.24	1.16	-	-	0.75	0.33	-	0.4	1.8	-
WIT 6-05	0.2	7.74	4.16	1.12	-	-	0.83	0.37	-	0.4	1.8	-
WIT 6-06	0.2	7.79	4.16	1.08	-	-	0.80	0.41	-	0.5	1.9	-
WIT 6-07	0.2	7.80	4.20	1.07	-	-	0.75	0.42	-	0.5	2.0	-
WIT 6-08	0.2	7.77	4.11	1.06	-	-	0.84	0.43	-	0.5	1.8	-
WIT 6-09	0.5	7.72	4.32	1.16	-	-	0.62	0.34	-	0.7	1.8	-
WIT 6-10	0.5	7.70	4.37	1.15	-	-	0.58	0.35	-	0.7	1.8	-
WIT 6-11	0.5	7.68	4.32	1.17	-	-	0.62	0.33	-	0.7	1.7	-
WIT 6-12	0.5	7.65	4.32	1.15	-	-	0.63	0.35	-	0.7	1.6	-
WIT 6-13	0.5	7.75	4.31	1.15	-	-	0.63	0.35	-	0.7	2.0	-
WIT 6-14	0.1	7.80	3.87	0.96	-	-	1.06	0.55	-	0.2	1.6	-
WIT 6-15	0.1	7.78	3.90	0.93	-	-	1.02	0.57	-	0.3	1.5	-
WIT 6-16	0.1	7.82	3.85	0.91	-	-	1.09	0.59	-	0.3	1.6	-
WIT 6-17	0.1	7.81	3.85	0.94	-	-	1.00	0.58	-	0.3	1.6	-
WIT 6-18	0.1	7.78	3.81	0.92	-	-	1.09	0.60	-	0.3	1.5	-
WIT 6-19	0.1	7.81	3.77	0.88	-	-	1.17	0.62	-	0.3	1.5	-
WIT 6-20	0.1	7.79	3.78	0.89	-	-	1.30	0.57	-	0.3	1.5	-
WIT 6-21	0.9	7.75	4.26	1.13	-	-	0.65	0.38	-	1.3	1.9	-
WIT 6-22	0.9	7.76	4.27	1.15	-	-	0.71	0.34	-	1.2	2.0	-
WIT 6-23	0.9	7.76	4.32	1.14	-	-	0.58	0.37	-	1.3	2.0	-
WIT 6-24	0.9	7.75	4.33	1.17	-	-	0.62	0.33	-	1.2	2.0	-

This is a preprint, the final version is subject to change, of the American Mineralogist (MSA)
Cite as Authors (Year) Title. American Mineralogist, in press.
DOI: http://dx.doi.org/10.2138/am-2018-6232

Sample	flowrate [ml/min]	pH [50°C]	total alkalinity [meq/l]	Ba^{2+} [mM]	Mg^{2+} [mM]	Mg:Ba	Δ total alkalinity [meq/l]	Δ Ba^{2+} [mM]	Δ Mg^{2+} [mM]	Rate [10^{-7} mol/m^2s^{-1}]	Ω witherite	Ω norsethite
WIT 6-25	0.9	7.75	4.37	1.19	-	-	0.59	0.30	-	1.1	2.0	-
WIT 6-26	0.9	7.77	4.36	1.18	-	-	0.57	0.32	-	1.1	2.1	-
WIT 7-1	0.2	8.50	11.38	0.07	-	-	0.82	0.23	-	0.2	1.5	-
WIT 7-2	0.2	8.49	11.50	0.07	-	-	0.70	0.23	-	0.2	1.6	-
WIT 7-3	0.2	8.42	11.74	0.05	-	-	0.47	0.24	-	0.2	1.1	-
WIT 7-4	0.2	8.41	11.67	0.05	-	-	0.54	0.24	-	0.2	1.1	-
WIT 7-5	0.2	8.50	11.78	0.06	-	-	0.42	0.23	-	0.2	1.5	-
WIT 7-6	0.2	8.48	11.91	0.06	-	-	0.29	0.24	-	0.2	1.4	-
WIT 7-7	0.2	8.52	11.93	0.06	-	-	0.28	0.23	-	0.2	1.6	-
WIT 7-8	0.2	8.52	11.98	0.06	-	-	0.22	0.24	-	0.2	1.5	-
WIT 7-9	0.2	8.54	11.95	0.06	-	-	0.25	0.24	-	0.2	1.6	-
WIT 7-10	0.2	8.52	11.79	0.06	-	-	0.41	0.24	-	0.2	1.4	-
WIT 7-11	0.2	8.59	12.10	0.06	-	-	0.10	0.23	-	0.2	1.8	-
WIT 7-12	0.2	8.52	11.95	0.06	-	-	0.26	0.24	-	0.2	1.5	-
WIT 7-13	0.2	8.50	11.83	0.06	-	-	0.37	0.24	-	0.2	1.4	-
WIT 7-14	0.2	8.52	11.92	0.06	-	-	0.28	0.24	-	0.2	1.5	-
WIT 7-15	0.2	8.53	11.92	0.05	-	-	0.28	0.25	-	0.2	1.3	-
WIT 7-16	0.2	8.53	11.83	0.06	-	-	0.37	0.24	-	0.2	1.4	-
WIT 7-18	0.4	8.36	11.79	0.08	-	-	0.41	0.21	-	0.4	1.5	-
WIT 7-19	0.4	8.36	11.77	0.09	-	-	0.43	0.21	-	0.3	1.5	-
WIT 7-20	0.4	8.38	11.84	0.09	-	-	0.37	0.21	-	0.3	1.7	-
WIT 7-21	0.4	8.41	11.81	0.09	-	-	0.39	0.21	-	0.3	1.8	-
WIT 7-22	0.4	8.38	11.73	0.08	-	-	0.48	0.22	-	0.4	1.5	-
WIT 7-23	0.4	8.42	11.74	0.08	-	-	0.46	0.22	-	0.4	1.6	-
WIT 7-24	0.4	8.39	11.85	0.09	-	-	0.35	0.21	-	0.3	1.7	-
WIT 7-25	0.4	8.37	11.81	0.09	-	-	0.40	0.21	-	0.0	1.7	-
WIT 7-26	0.4	8.37	11.77	0.08	-	-	0.43	0.22	-	0.3	1.5	-
WIT 7-27	0.4	8.42	11.85	0.08	-	-	0.35	0.22	-	0.3	1.6	-
WIT 7-28	0.4	8.40	11.81	0.08	-	-	0.40	0.22	-	0.3	1.5	-
WIT 7-29	0.4	8.39	11.89	0.10	-	-	0.17	0.16	-	0.2	1.9	-
WIT 7-31	0.8	8.26	11.93	0.14	-	-	0.14	0.12	-	0.3	2.0	-
WIT 7-32	0.8	8.26	11.93	0.12	-	-	0.13	0.13	-	0.4	1.8	-
WIT 7-33	0.8	8.26	11.90	0.12	-	-	0.17	0.13	-	0.4	1.8	-
WIT 7-34	0.8	8.26	11.91	0.13	-	-	0.15	0.12	-	0.4	1.9	-
WIT 7-35	0.8	8.27	11.96	0.12	-	-	0.11	0.13	-	0.4	1.9	-
WIT 7-36	0.8	8.27	12.00	0.13	-	-	0.07	0.12	-	0.3	2.0	-
WIT 7-37	0.8	8.24	11.99	0.14	-	-	0.08	0.11	-	0.3	2.0	-

This is a preprint, the final version is subject to change, of the American Mineralogist (MSA)
Cite as Authors (Year) Title. American Mineralogist, in press.
DOI: http://dx.doi.org/10.2138/am-2018-6232

Sample	flowrate [ml/min]	pH [50°C]	total alkalinity [meq/l]	Ba^{2+} [mM]	Mg^{2+} [mM]	Mg:Ba	Δ total alkalinity [meq/l]	Δ Ba^{2+} [mM]	Δ Mg^{2+} [mM]	Rate [10^{-7} mol/m^2s^{-1}]	Ω witherite	Ω norsethite
WIT 7-38	0.8	8.26	11.98	0.12	-	-	0.09	0.13	-	0.4	1.8	-
WIT 7-39	0.7	8.30	11.93	0.13	-	-	0.13	0.13	-	0.3	2.0	-
WIT 7-40	0.8	8.30	11.91	0.13	-	-	0.16	0.12	-	0.3	2.1	-
WIT 8-1	0.1	8.06	6.56	0.26	-	-	3.40	0.72	-	0.4	1.3	-
WIT 8-2	0.1	8.07	8.56	0.26	-	-	1.40	0.72	-	0.3	1.7	-
WIT 8-3	0.1	8.04	8.59	0.27	-	-	1.36	0.71	-	0.3	1.7	-
WIT 8-4	0.1	8.00	8.57	0.26	-	-	1.38	0.72	-	0.3	1.5	-
WIT 8-5	0.1	8.06	8.78	0.25	-	-	1.18	0.74	-	0.3	1.7	-
WIT 8-6	0.1	8.08	8.57	0.25	-	-	1.38	0.73	-	0.3	1.7	-
WIT 8-7	0.1	8.02	8.64	0.27	-	-	1.32	0.71	-	0.3	1.6	-
WIT 8-8	0.1	8.04	8.54	0.24	-	-	1.41	0.75	-	0.3	1.5	-
WIT 8-9	0.5	8.07	8.65	0.29	-	-	1.30	0.69	-	1.2	2.0	-
WIT 8-10	0.5	8.08	8.76	0.33	-	-	1.19	0.65	-	1.1	2.3	-
WIT 8-11	0.5	8.08	8.77	0.33	-	-	1.19	0.65	-	1.1	2.3	-
WIT 8-12	0.5	7.98	8.89	0.44	-	-	1.06	0.54	-	0.9	2.5	-
WIT 8-13	0.5	7.96	8.89	0.45	-	-	1.07	0.54	-	0.9	2.4	-
WIT 8-14	0.5	7.93	8.80	0.43	-	-	1.15	0.55	-	0.9	2.2	-
WIT 8-15	0.5	8.03	8.79	0.41	-	-	1.16	0.58	-	0.9	2.6	-
WIT 8-16	0.9	8.00	8.85	0.44	-	-	1.10	0.54	-	1.4	2.6	-
WIT 8-17	1.0	8.00	8.89	0.44	-	-	1.06	0.54	-	1.5	2.7	-
WIT 8-18	1.0	8.00	8.89	0.45	-	-	1.06	0.53	-	1.5	2.7	-
WIT 8-19	0.9	7.87	8.89	0.47	-	-	1.06	0.51	-	1.3	2.1	-
WIT 8-20	1.0	7.86	8.88	0.48	-	-	1.07	0.51	-	1.4	2.1	-
WIT 8-21	1.0	7.86	8.89	0.48	-	-	1.07	0.50	-	1.4	2.1	-
WIT 8-22	1.3	8.03	8.90	0.50	-	-	1.05	0.48	-	1.7	3.2	-
WIT 8-23	1.4	8.02	8.88	0.49	-	-	1.07	0.49	-	1.7	3.1	-
WIT 8-24	1.4	8.02	8.88	0.49	-	-	1.07	0.50	-	1.8	3.0	-
WIT 8-25	1.7	8.01	8.88	0.51	-	-	1.07	0.47	-	2.0	3.1	-
WIT 8-26	1.6	7.96	8.96	0.50	-	-	1.00	0.48	-	2.0	2.7	-
WIT 8-27	1.6	8.01	8.88	0.51	-	-	1.07	0.47	-	2.0	3.1	-
WIT 8-28	1.6	7.96	8.86	0.51	-	-	1.10	0.47	-	2.0	2.8	-
WIT 8-29	1.9	8.07	8.92	0.51	-	-	1.04	0.47	-	2.3	3.6	-
WIT 8-30	1.9	8.06	8.89	0.52	-	-	1.06	0.46	-	2.1	3.5	-
WIT 8-31	1.9	8.06	8.90	0.52	-	-	1.06	0.46	-	2.1	3.6	-
WIT 8-32	1.7	8.06	8.58	0.53	-	-	1.37	0.45	-	1.9	3.5	-
WIT 8-33	1.8	8.07	8.85	0.51	-	-	1.10	0.47	-	2.2	3.5	-
WIT 8-34	1.9	8.06	8.89	0.51	-	-	1.06	0.47	-	2.2	3.5	-

This is a preprint, the final version is subject to change, of the American Mineralogist (MSA)
Cite as Authors (Year) Title. American Mineralogist, in press.
DOI: http://dx.doi.org/10.2138/am-2018-6232

Sample	flowrate [ml/min]	pH [50°C]	total alkalinity [meq/l]	Ba^{2+} [mM]	Mg^{2+} [mM]	Mg:Ba	Δ total alkalinity [meq/l]	Δ Ba^{2+} [mM]	Δ Mg^{2+} [mM]	Rate [10^{-7} mol/m^2s^{-1}]	Ω witherite	Ω norsethite
WIT 8-35	1.9	8.11	8.87	0.51	-	-	1.09	0.47	-	2.2	3.8	-
WIT 8-36	1.9	8.06	8.86	0.50	-	-	1.09	0.48	-	2.2	3.4	-
WIT 8-37	1.1	7.98	8.30	0.55	-	-	1.66	0.43	-	1.2	2.9	-
WIT 8-38	1.8	8.05	8.06	0.59	-	-	1.90	0.39	-	1.6	3.6	-
WIT 8-39	1.9	8.11	8.83	0.52	-	-	1.12	0.47	-	2.1	3.9	-
WIT 8-40	1.9	8.03	8.82	0.52	-	-	1.14	0.46	-	2.0	3.3	-
WIT 11-1	0.1	8.05	3.94	0.26	-	-	5.98	0.78	-	0.6	0.8	-
WIT 11-2	0.1	7.99	8.18	0.28	-	-	1.74	0.77	-	0.5	1.5	-
WIT 11-3	0.1	7.96	8.21	0.28	-	-	1.71	0.77	-	0.5	1.4	-
WIT 11-4	0.1	8.05	8.34	0.24	-	-	1.58	0.80	-	0.5	1.5	-
WIT 11-5	0.1	8.02	8.32	0.27	-	-	1.60	0.78	-	0.5	1.6	-
WIT 11-6	0.2	7.94	8.48	0.33	-	-	1.44	0.72	-	0.8	1.7	-
WIT 11-7	0.1	8.04	8.59	0.28	-	-	1.32	0.77	-	0.5	1.8	-
WIT 11-8	0.2	8.01	9.08	0.27	-	-	0.83	0.78	-	0.9	1.7	-
WIT 11-9	0.5	8.07	8.68	0.42	-	-	1.24	0.62	-	1.4	2.9	-
WIT 11-10	0.5	8.04	8.72	0.42	-	-	1.19	0.62	-	1.4	2.7	-
WIT 11-11	0.5	8.04	8.69	0.43	-	-	1.23	0.62	-	1.4	2.8	-
WIT 11-12	0.5	8.04	8.59	0.43	-	-	1.33	0.62	-	1.4	2.7	-
WIT 11-13	0.7	8.07	8.70	0.46	-	-	1.22	0.58	-	1.9	3.2	-
WIT 11-14	0.7	8.05	8.70	0.47	-	-	1.21	0.58	-	1.9	3.0	-
WIT 11-15	0.6	8.06	8.77	0.46	-	-	1.14	0.58	-	1.6	3.1	-
WIT 11-16	0.7	8.04	8.79	0.47	-	-	1.13	0.58	-	1.9	3.0	-
WIT 11-17	1.0	8.10	8.82	0.48	-	-	1.09	0.56	-	2.4	3.6	-
WIT 11-18	1.0	8.07	8.81	0.48	-	-	1.10	0.56	-	2.4	3.4	-
WIT 11-19	0.9	8.05	8.82	0.48	-	-	1.10	0.57	-	2.3	3.2	-
WIT 11-20	1.1	8.08	8.77	0.47	-	-	1.14	0.57	-	2.8	3.3	-
WIT 11-21	1.0	8.11	8.81	0.41	-	-	1.10	0.63	-	2.6	3.1	-
WIT 12-1	0.2	8.03	4.40	0.68	-	-	0.89	0.34	-	0.5	2.2	-
WIT 12-2	0.2	8.02	4.44	0.63	-	-	0.84	0.38	-	0.5	2.1	-
WIT 12-3	0.2	7.97	4.55	0.64	-	-	0.73	0.38	-	0.5	1.9	-
WIT 12-4	0.2	7.97	4.55	0.64	-	-	0.73	0.38	-	0.5	1.9	-
WIT 12-5	0.2	7.97	4.54	0.64	-	-	0.74	0.37	-	0.5	1.9	-
WIT 12-6	0.5	8.05	4.75	0.72	-	-	0.53	0.30	-	1.1	2.6	-
WIT 12-7	0.5	8.04	4.77	0.71	-	-	0.51	0.31	-	1.2	2.6	-
WIT 12-8	0.5	8.05	4.74	0.73	-	-	0.54	0.29	-	1.1	2.6	-
WIT 12-9	0.5	8.04	4.74	0.72	-	-	0.54	0.30	-	1.1	2.6	-
WIT 12-10	0.5	8.04	4.73	0.72	-	-	0.55	0.30	-	1.1	2.6	-

This is a preprint, the final version is subject to change, of the American Mineralogist (MSA)
Cite as Authors (Year) Title. American Mineralogist, in press.
DOI: http://dx.doi.org/10.2138/am-2018-6232

Sample	flowrate [ml/min]	pH [50°C]	total alkalinity [meq/l]	Ba^{2+} [mM]	Mg^{2+} [mM]	Mg:Ba	Δ total alkalinity [meq/l]	Δ Ba^{2+} [mM]	Δ Mg^{2+} [mM]	Rate [10^{-7} mol/m^2s^{-1}]	Ω witherite	Ω norsethite
WIT 12-11	1.0	8.15	4.84	0.74	-	-	0.44	0.28	-	2.0	3.4	-
WIT 12-12	0.9	8.14	4.83	0.74	-	-	0.45	0.28	-	2.0	3.4	-
WIT 12-13	0.9	8.14	4.87	0.75	-	-	0.41	0.27	-	2.0	3.4	-
WIT 12-14	1.0	8.14	4.84	0.74	-	-	0.44	0.27	-	2.0	3.4	-
WIT 12-15	1.0	8.14	4.82	0.75	-	-	0.46	0.27	-	2.0	3.4	-
WIT 12-16	0.6	8.09	4.74	0.72	-	-	0.54	0.29	-	1.4	2.9	-
WIT 12-17	0.6	8.09	4.74	0.72	-	-	0.55	0.30	-	1.4	2.9	-
WIT 12-18	0.6	8.10	4.75	0.72	-	-	0.54	0.30	-	1.4	2.9	-
WIT 12-19	0.6	8.10	4.74	0.72	-	-	0.54	0.30	-	1.4	2.9	-
WITMg 7-1	0.2	8.60	11.30	0.04	0.03	0.79	0.98	0.25	0.00	0.22	1.1	0.3
WITMg 7-2	0.2	8.59	11.40	0.04	0.03	0.92	0.88	0.25	0.00	0.22	1.0	0.3
WITMg 7-3	0.2	8.54	11.50	0.04	0.03	0.77	0.77	0.25	0.00	0.21	1.0	0.3
WITMg 7-4	0.2	8.51	11.62	0.05	0.03	0.74	0.66	0.25	0.00	0.21	1.0	0.3
WITMg 7-5	0.2	8.59	11.61	0.05	0.03	0.71	0.66	0.25	0.00	0.21	1.2	0.4
WITMg 7-6	0.2	8.57	11.84	0.05	0.03	0.74	0.44	0.25	0.00	0.21	1.2	0.4
WITMg 7-7	0.2	8.62	11.86	0.05	0.03	0.75	0.42	0.25	0.00	0.21	1.3	0.4
WITMg 7-8	0.2	8.62	11.79	0.05	0.03	0.74	0.49	0.25	0.00	0.23	1.3	0.4
WITMg 7-9	0.2	8.64	11.71	0.05	0.03	0.74	0.57	0.25	0.00	0.20	1.4	0.4
WITMg 7-10	0.2	8.63	11.72	0.04	0.04	0.94	0.56	0.25	0.00	0.21	1.1	0.3
WITMg 7-11	0.1	8.59	11.61	0.05	0.03	0.71	0.67	0.24	0.00	0.20	1.2	0.4
WITMg 7-12	0.1	8.63	11.68	0.05	0.04	0.76	0.59	0.25	0.00	0.20	1.3	0.4
WITMg 7-13	0.1	8.61	11.86	0.05	0.03	0.73	0.42	0.24	0.00	0.20	1.3	0.4
WITMg 7-14	0.1	8.61	11.90	0.05	0.03	0.72	0.37	0.25	0.00	0.20	1.3	0.4
WITMg 7-15	0.1	8.65	11.92	0.04	0.03	0.80	0.35	0.25	0.00	0.20	1.2	0.4
WITMg 7-16	0.1	8.63	11.69	0.05	0.03	0.73	0.59	0.25	0.00	0.19	1.3	0.4
WITMg 7-18	0.4	8.47	11.66	0.08	0.03	0.44	0.62	0.22	0.00	0.42	1.5	0.4
WITMg 7-19	0.4	8.47	11.71	0.07	0.04	0.49	0.57	0.22	0.00	0.42	1.5	0.4
WITMg 7-20	0.4	8.47	11.67	0.07	0.03	0.49	0.61	0.22	0.00	0.42	1.5	0.4
WITMg 7-21	0.4	8.50	11.67	0.07	0.04	0.50	0.61	0.22	0.00	0.42	1.6	0.4
WITMg 7-22	0.4	8.48	11.56	0.07	0.03	0.48	0.71	0.22	0.00	0.42	1.5	0.4
WITMg 7-23	0.4	8.50	11.75	0.08	0.03	0.40	0.53	0.21	0.00	0.40	1.8	0.5
WITMg 7-24	0.4	8.49	11.73	0.07	0.03	0.47	0.55	0.22	0.00	0.42	1.5	0.4
WITMg 7-25	0.4	8.48	11.73	0.08	0.03	0.45	0.55	0.22	0.00	0.00	1.6	0.4
WITMg 7-26	0.4	8.47	11.73	0.08	0.03	0.43	0.55	0.21	0.00	0.40	1.7	0.4
WITMg 7-27	0.4	8.51	11.77	0.07	0.03	0.51	0.51	0.23	0.00	0.43	1.5	0.4
WITMg 7-28	0.4	8.50	11.80	0.08	0.03	0.45	0.48	0.22	-0.01	0.41	1.7	0.4
WITMg 7-29	0.4	8.49	11.84	0.07	0.03	0.52	0.20	0.18	-0.01	0.33	1.5	0.4

This is a preprint, the final version is subject to change, of the American Mineralogist (MSA)
Cite as Authors (Year) Title. American Mineralogist, in press.
DOI: http://dx.doi.org/10.2138/am-2018-6232

Sample	flowrate [ml/min]	pH [50°C]	total alkalinity [meq/l]	Ba^{2+} [mM]	Mg^{2+} [mM]	Mg:Ba	Δ total alkalinity [meq/l]	Δ Ba^{2+} [mM]	Δ Mg^{2+} [mM]	Rate [10^{-7} mol/m^2s^{-1}]	Ω witherite	Ω norsethite
WITMg 7-31	0.7	8.44	11.72	0.11	0.03	0.24	0.32	0.14	0.00	0.50	2.1	0.3
WITMg 7-32	0.7	8.47	11.79	0.10	0.03	0.27	0.25	0.14	0.00	0.53	2.0	0.4
WITMg 7-33	0.7	8.47	11.77	0.12	0.02	0.21	0.27	0.12	0.00	0.45	2.5	0.4
WITMg 7-34	0.7	8.46	11.76	0.10	0.03	0.27	0.28	0.14	0.00	0.52	2.0	0.4
WITMg 7-35	0.7	8.48	11.77	0.13	0.03	0.19	0.27	0.11	0.00	0.41	2.8	0.5
WITMg 7-36	0.7	8.46	11.79	0.11	0.02	0.23	0.25	0.13	0.00	0.48	2.2	0.4
WITMg 7-37	0.7	8.44	11.76	0.10	0.02	0.25	0.28	0.14	0.00	0.52	2.0	0.3
WITMg 7-38	0.7	8.45	11.78	0.10	0.03	0.25	0.26	0.14	0.00	0.48	2.1	0.3
WITMg 7-39	0.7	8.48	11.71	0.09	0.03	0.29	0.33	0.16	0.00	0.55	1.9	0.3
WITMg 7-40	0.7	8.48	11.78	0.10	0.02	0.26	0.26	0.15	0.00	0.52	2.1	0.4
WITMg 8-1	0.4	7.55	7.26	0.73	17.11	23.5	2.68	1.30	3.03	-	1.3	96.8
WITMg 8-2	0.5	7.47	7.47	0.82	18.12	22.0	2.48	1.21	2.03	-	1.1	69.5
WITMg 8-3	0.4	7.47	7.56	0.83	18.10	21.9	2.39	1.21	2.04	-	1.2	74.4
WITMg 8-5	0.4	7.23	7.51	0.79	19.60	24.8	2.44	1.24	0.54	-	0.6	24.8
WITMg 8-6	0.4	7.22	7.50	0.89	19.83	22.3	2.44	1.14	0.31	-	0.7	25.5
WITMg 8-7	0.4	7.16	7.32	1.12	19.64	17.5	2.62	0.91	0.50	-	0.7	24.4
WITMg 8-8	0.4	7.15	7.26	1.15	19.39	16.9	2.69	0.88	0.76	-	0.7	23.3
WITMg 8-9	0.4	7.15	7.17	1.29	19.13	14.9	2.78	0.75	1.01	-	0.8	24.2
WITMg 8-10	0.4	7.05	6.94	1.42	19.10	13.5	3.00	0.61	1.04	-	0.7	15.9
WITMg 8-11	0.4	7.05	6.99	1.44	19.07	13.2	2.96	0.59	1.07	-	0.7	16.3
WITMg 8-12	0.4	7.04	6.98	1.41	18.97	13.5	2.96	0.62	1.18	-	0.7	15.2
WITMg 8-13	0.4	7.05	6.98	1.40	19.38	13.8	2.97	0.63	0.77	-	0.7	16.0
WITMg 8-14	0.4	7.04	7.46	1.63	18.99	11.6	2.49	0.40	1.15	-	0.8	19.9
WITMg 8-15	0.4	7.02	7.46	1.57	19.38	12.3	2.48	0.46	0.77	-	0.8	17.7
WITMg 8-17	0.4	7.00	7.12	1.69	18.99	11.3	2.83	0.35	1.15	-	0.7	15.6
WITMg 8-18	0.4	7.00	7.26	1.67	19.13	11.5	2.69	0.36	1.01	-	0.7	16.1
WITMg 8-19	0.5	7.00	7.14	1.70	18.98	11.2	2.80	0.34	1.17	-	0.7	15.1
WITMg 8-20	0.7	7.01	7.40	1.70	19.00	11.2	2.55	0.34	1.14	-	0.8	17.7
WITMg 8-21	0.6	7.04	7.48	1.57	18.95	12.1	2.46	0.46	1.19	-	0.8	19.2
WITMg 8-22	0.6	7.03	7.41	1.17	19.85	17.0	2.54	0.86	0.29	-	0.6	13.8
WITMg 8-23	0.7	7.03	7.41	1.53	19.22	12.6	2.54	0.50	0.93	-	0.7	17.7
WITMg 8-24	0.7	7.03	7.46	1.57	19.26	12.2	2.48	0.46	0.89	-	0.8	18.5
WITMg 8-25	0.6	7.03	7.64	1.54	19.35	12.6	2.31	0.49	0.79	-	0.8	18.9
WITMg 8-26	1.1	7.05	7.63	1.60	19.26	12.0	2.32	0.43	0.88	-	0.8	21.5
WITMg 8-27	1.1	7.05	7.66	1.54	19.44	12.6	2.29	0.49	0.70	-	0.8	21.0
WITMg 8-28	1.1	7.04	7.65	1.53	19.54	12.8	2.29	0.50	0.60	-	0.8	19.9
WITMg 8-29	1.1	7.06	7.71	1.59	19.38	12.2	2.24	0.45	0.76	-	0.9	22.8

This is a preprint, the final version is subject to change, of the American Mineralogist (MSA)
Cite as Authors (Year) Title. American Mineralogist, in press.
DOI: http://dx.doi.org/10.2138/am-2018-6232

Sample	flowrate [ml/min]	pH [50°C]	total alkalinity [meq/l]	Ba^{2+} [mM]	Mg^{2+} [mM]	Mg:Ba	Δ total alkalinity [meq/l]	Δ Ba^{2+} [mM]	Δ Mg^{2+} [mM]	Rate [10^{-7} mol/m^2s^{-1}]	Ω witherite	Ω norsethite
WITMg 8-30	1.1	7.06	7.73	1.57	19.38	12.3	2.22	0.46	0.76	-	0.9	22.7
WITMg 8-31	1.1	7.05	7.69	1.54	19.67	12.8	2.26	0.50	0.47	-	0.8	21.1
WITMg 8-32	1.1	7.05	7.69	1.57	19.39	12.3	2.26	0.46	0.75	-	0.8	21.4
WITMg 9-1	0.1	7.97	8.64	0.18	0.96	5.21	1.56	0.79	0.04	0.5	1.4	3.5
WITMg 9-2	0.1	7.96	8.74	0.18	1.00	5.58	1.46	0.80	0.01	0.5	1.4	3.4
WITMg 9-3	0.1	7.97	8.78	0.18	1.00	5.69	1.42	0.80	0.00	0.5	1.4	3.5
WITMg 9-4	0.1	7.97	8.73	0.18	0.98	5.37	1.47	0.79	0.02	0.5	1.4	3.6
WITMg 9-5	0.1	7.97	8.73	0.18	0.98	5.36	1.46	0.79	0.03	0.5	1.4	3.6
WITMg 9-6	0.1	7.96	8.74	0.18	1.02	5.71	1.46	0.80	-0.01	0.5	1.4	3.5
WITMg 9-7	0.1	8.01	8.56	0.13	1.00	7.49	1.64	0.84	0.00	0.3	1.1	3.1
WITMg 9-8	0.1	8.01	8.54	0.13	1.02	7.63	1.66	0.84	-0.01	0.3	1.1	3.1
WITMg 9-9	0.6	7.97	8.86	0.35	1.04	2.96	1.33	0.63	-0.03	1.1	2.8	7.4
WITMg 9-10	0.6	8.02	8.92	0.34	1.06	3.15	1.28	0.64	-0.06	1.1	3.0	9.1
WITMg 9-11	0.6	8.03	8.84	0.34	1.03	2.99	1.36	0.63	-0.02	1.1	3.1	9.3
WITMg 9-12	0.6	8.01	8.85	0.33	1.02	3.08	1.35	0.64	-0.02	1.1	2.9	8.2
WITMg 9-13	0.6	8.02	8.87	0.34	1.02	2.99	1.33	0.64	-0.01	1.1	3.0	8.8
WITMg 9-14	1.1	7.99	8.93	0.38	0.91	2.38	1.27	0.59	0.09	1.9	3.2	7.9
WITMg 9-15	1.1	7.97	8.92	0.38	0.99	2.59	1.28	0.60	0.02	1.8	3.0	7.7
WITMg 9-16	1.1	7.96	8.89	0.38	0.99	2.60	1.30	0.60	0.01	1.8	3.0	7.4
WITMg 9-17	1.1	7.96	8.92	0.38	0.99	2.63	1.28	0.60	0.01	1.9	2.9	7.3
WITMg 9-18	1.1	7.96	8.93	0.38	0.99	2.61	1.27	0.60	0.02	1.9	3.0	7.4
WITMg 9-19	0.4	8.08	8.81	0.26	0.98	3.78	1.39	0.72	0.03	0.7	2.6	8.2
WITMg 9-20	0.4	8.05	8.77	0.26	0.99	3.89	1.43	0.72	0.01	0.7	2.4	7.2
WITMg 9-21	0.4	8.06	8.79	0.26	0.97	3.78	1.41	0.72	0.04	0.7	2.5	7.4
WITMg 9-22	0.4	8.04	8.80	0.24	1.00	4.09	1.40	0.73	0.01	0.8	2.3	6.7
WITMg 9-23	1.4	8.02	8.93	0.38	0.98	2.57	1.27	0.60	0.03	2.3	3.4	9.5
WITMg 9-24	1.5	8.03	8.91	0.38	1.00	2.64	1.29	0.60	0.01	2.4	3.4	10.0
WITMg 9-25	1.5	8.03	8.89	0.38	0.99	2.59	1.30	0.60	0.02	2.4	3.4	10.0
WITMg 9-26	1.4	8.05	8.88	0.38	0.99	2.59	1.32	0.59	0.01	2.3	3.6	10.9
WITMg 9-27	0.1	8.00	8.37	0.16	0.97	6.11	1.82	0.82	0.04	0.3	1.3	3.3
WITMg 9-28	0.1	8.07	8.51	0.16	0.97	6.19	1.69	0.82	0.04	0.2	1.5	4.5
WITMg 9-29	0.1	8.06	8.51	0.18	0.96	5.27	1.69	0.80	0.05	0.2	1.7	4.9
WITMg 9-30	0.1	8.08	8.40	0.14	1.00	7.11	1.80	0.84	0.00	0.3	1.4	4.2
WITMg 10-1	1.0	7.81	4.70	1.68	2.12	1.26	0.70	0.38	0.00	2.1	3.4	5.1
WITMg 10-2	1.0	7.81	4.70	1.71	2.05	1.20	0.70	0.34	0.07	1.9	3.4	5.0
WITMg 10-3	1.0	7.82	4.73	1.71	2.11	1.23	0.67	0.35	0.02	1.9	3.5	5.6
WITMg 10-4	1.0	7.81	4.73	1.69	2.15	1.27	0.67	0.37	-0.03	2.0	3.4	5.3

This is a preprint, the final version is subject to change, of the American Mineralogist (MSA)
Cite as Authors (Year) Title. American Mineralogist, in press.
DOI: http://dx.doi.org/10.2138/am-2018-6232

Sample	flowrate [ml/min]	pH [50°C]	total alkalinity [meq/l]	Ba^{2+} [mM]	Mg^{2+} [mM]	Mg:Ba	Δ total alkalinity [meq/l]	Δ Ba^{2+} [mM]	Δ Mg^{2+} [mM]	Rate [10^{-7} mol/m^2s^{-1}]	Ω witherite	Ω norsethite
WITMg 10-5	1.0	7.82	4.73	1.70	2.19	1.29	0.67	0.36	-0.07	1.9	3.5	5.6
WITMg 10-6	2.0	7.85	4.84	1.76	2.02	1.15	0.56	0.30	0.10	3.1	4.0	6.5
WITMg 10-7	2.0	7.84	4.82	1.76	2.04	1.16	0.58	0.30	0.08	3.1	3.9	6.2
WITMg 10-8	1.9	7.83	4.76	1.75	2.03	1.16	0.64	0.31	0.09	3.1	3.7	5.8
WITMg 10-9	2.0	7.82	4.77	1.75	2.00	1.14	0.63	0.31	0.13	3.1	3.7	5.5
WITMg 10-10	1.9	7.82	4.76	1.71	2.04	1.19	0.64	0.35	0.08	3.5	3.6	5.5
WITMg 10-11	0.5	7.78	4.39	1.52	2.08	1.37	1.01	0.54	0.04	1.4	2.7	3.6
WITMg 10-12	0.5	7.78	4.31	1.30	2.17	1.67	1.09	0.76	-0.05	2.0	2.3	3.0
WITMg 10-13	0.5	7.79	4.32	1.47	2.08	1.41	1.08	0.59	0.04	1.5	2.6	3.4
WITMg 10-14	0.5	7.80	4.31	1.49	2.07	1.40	1.09	0.57	0.05	1.5	2.7	3.6
WITMg 10-15	0.5	7.79	4.42	1.52	2.06	1.35	0.98	0.54	0.06	1.4	2.8	3.7
WITMg 10-16	0.2	7.82	3.89	1.26	2.05	1.63	1.51	0.80	0.07	0.7	2.2	2.8
WITMg 10-17	0.2	7.83	3.79	1.20	2.17	1.81	1.61	0.86	-0.05	0.8	2.1	2.8
WITMg 10-18	0.2	7.85	3.97	1.17	2.20	1.87	1.43	0.89	-0.07	1.0	2.2	3.2
WITMg 10-19	0.1	7.86	2.98	0.84	2.06	2.45	2.42	1.22	0.06	0.5	1.2	1.3
WITMg 11-1	0.1	8.09	4.00	0.28	0.02	0.05	5.80	0.78	0.09	0.6	1.5	0.0
WITMg 11-2	0.1	7.89	8.16	0.31	0.11	0.35	1.64	0.76	0.00	0.5	2.0	0.4
WITMg 11-3	0.1	7.89	8.29	0.31	0.11	0.37	1.51	0.76	-0.01	0.5	2.0	0.5
WITMg 11-4	0.1	7.89	8.37	0.28	0.11	0.38	1.43	0.79	0.00	0.5	1.8	0.4
WITMg 11-5	0.1	7.90	8.28	0.29	0.10	0.36	1.52	0.78	0.00	0.4	1.9	0.4
WITMg 11-6	0.3	7.90	8.45	0.33	0.14	0.43	1.35	0.74	-0.04	0.8	2.2	0.7
WITMg 11-7	0.2	7.90	8.42	0.35	0.13	0.38	1.38	0.72	-0.03	0.7	2.3	0.7
WITMg 11-8	0.2	7.90	8.43	0.34	0.12	0.36	1.37	0.72	-0.02	0.7	2.3	0.6
WITMg 11-9	0.5	7.90	8.55	0.43	0.14	0.32	1.25	0.63	-0.03	1.2	2.9	0.9
WITMg 11-10	0.5	7.90	8.55	0.44	0.13	0.30	1.25	0.62	-0.03	1.4	3.0	0.9
WITMg 11-11	0.5	7.89	8.62	0.45	0.12	0.28	1.18	0.62	-0.02	1.4	3.0	0.8
WITMg 11-12	0.5	7.89	8.70	0.46	0.13	0.27	1.10	0.61	-0.02	1.3	3.1	0.9
WITMg 11-13	0.7	7.89	8.82	0.47	0.15	0.32	0.98	0.60	-0.05	1.8	3.2	1.1
WITMg 11-14	0.7	7.89	8.66	0.49	0.14	0.28	1.14	0.58	-0.04	1.7	3.3	1.0
WITMg 11-15	0.6	7.89	8.73	0.50	0.13	0.26	1.07	0.56	-0.03	1.4	3.4	1.0
WITMg 11-16	0.7	7.89	8.76	0.50	0.13	0.26	1.04	0.56	-0.03	1.7	3.4	1.0
WITMg 11-17	1.0	7.89	8.83	0.51	0.14	0.28	0.97	0.55	-0.04	2.1	3.5	1.1
WITMg 11-18	1.0	7.90	8.81	0.45	0.20	0.44	0.99	0.61	-0.10	2.4	3.1	1.4
WITMg 11-19	0.9	7.90	8.79	0.52	0.13	0.26	1.01	0.54	-0.03	2.0	3.6	1.0
WITMg 11-20	1.0	7.90	8.77	0.52	0.14	0.26	1.03	0.55	-0.03	2.1	3.6	1.1
WITMg 11-21	1.0	7.90	8.78	0.51	0.14	0.27	1.02	0.56	-0.03	2.1	3.5	1.1
WITMg 12-1	0.2	7.90	4.38	0.65	2.75	4.24	0.95	0.35	0.23	0.4	1.5	0.1

This is a preprint, the final version is subject to change, of the American Mineralogist (MSA)
Cite as Authors (Year) Title. American Mineralogist, in press.
DOI: http://dx.doi.org/10.2138/am-2018-6232

Sample	flowrate [ml/min]	pH [50°C]	total alkalinity [meq/l]	Ba^{2+} [mM]	Mg^{2+} [mM]	Mg:Ba	Δ total alkalinity [meq/l]	Δ Ba^{2+} [mM]	Δ Mg^{2+} [mM]	Rate [10^{-7} mol/m^2s^{-1}]	Ω witherite	Ω norsethite
WITMg 12-2	0.2	7.90	4.41	0.67	2.81	4.20	0.91	0.32	0.17	0.4	1.5	0.2
WITMg 12-3	0.2	7.90	4.49	0.67	2.90	4.35	0.83	0.33	0.08	0.4	1.5	0.2
WITMg 12-4	0.2	7.90	4.51	0.69	2.83	4.11	0.81	0.30	0.15	0.4	1.6	0.2
WITMg 12-5	0.2	7.90	4.54	0.66	2.88	4.35	0.78	0.33	0.10	0.4	1.6	0.2
WITMg 12-6	0.5	7.89	4.75	0.77	2.91	3.76	0.57	0.22	0.07	0.7	1.9	0.2
WITMg 12-7	0.5	7.89	4.76	0.77	2.99	3.86	0.56	0.22	-0.01	0.7	1.9	0.2
WITMg 12-8	0.5	7.89	4.79	0.80	2.91	3.64	0.53	0.20	0.07	0.6	1.9	0.2
WITMg 12-9	0.5	7.89	4.76	0.79	2.91	3.69	0.56	0.21	0.07	0.7	1.9	0.2
WITMg 12-10	0.5	7.89	4.73	0.78	2.92	3.76	0.59	0.22	0.06	0.7	1.9	0.2
WITMg 12-11	0.8	7.93	4.82	0.82	2.93	3.58	0.51	0.18	0.05	1.0	2.2	0.3
WITMg 12-12	0.9	7.92	4.81	0.81	2.98	3.70	0.51	0.19	0.00	1.2	2.1	0.3
WITMg 12-13	0.9	7.92	4.79	0.84	2.91	3.46	0.53	0.15	0.07	1.0	2.2	0.3
WITMg 12-14	0.9	7.92	4.78	0.83	2.91	3.52	0.54	0.17	0.07	1.1	2.2	0.3
WITMg 12-15	0.9	7.92	4.79	0.82	2.95	3.60	0.53	0.18	0.03	1.1	2.1	0.3
WITMg 12-16	0.6	7.93	4.74	0.78	2.97	3.81	0.58	0.22	0.01	0.8	2.1	0.2
WITMg 12-17	0.6	7.93	4.74	0.78	2.99	3.81	0.58	0.21	-0.01	0.8	2.1	0.3
WITMg 12-18	0.6	7.93	4.75	0.79	2.96	3.75	0.57	0.20	0.02	0.8	2.1	0.3
WITMg 12-19	0.6	7.93	4.75	0.83	2.66	3.22	0.57	0.17	0.32	0.7	2.2	0.2

This is a preprint, the final version is subject to change, of the American Mineralogist (MSA)
Cite as Authors (Year) Title. American Mineralogist, in press.
DOI: http://dx.doi.org/10.2138/am-2018-6232

Figure 1

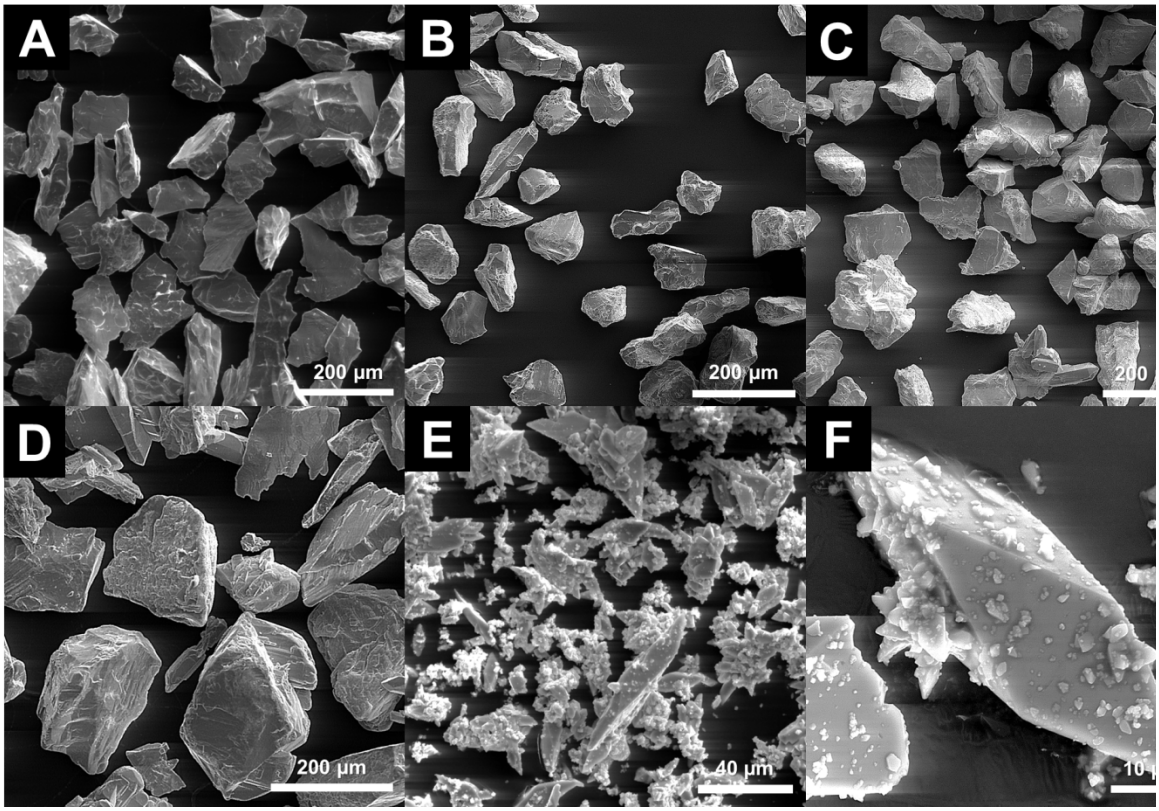

This is a preprint, the final version is subject to change, of the American Mineralogist (MSA)
Cite as Authors (Year) Title. American Mineralogist, in press.
DOI: http://dx.doi.org/10.2138/am-2018-6232

Figure 2

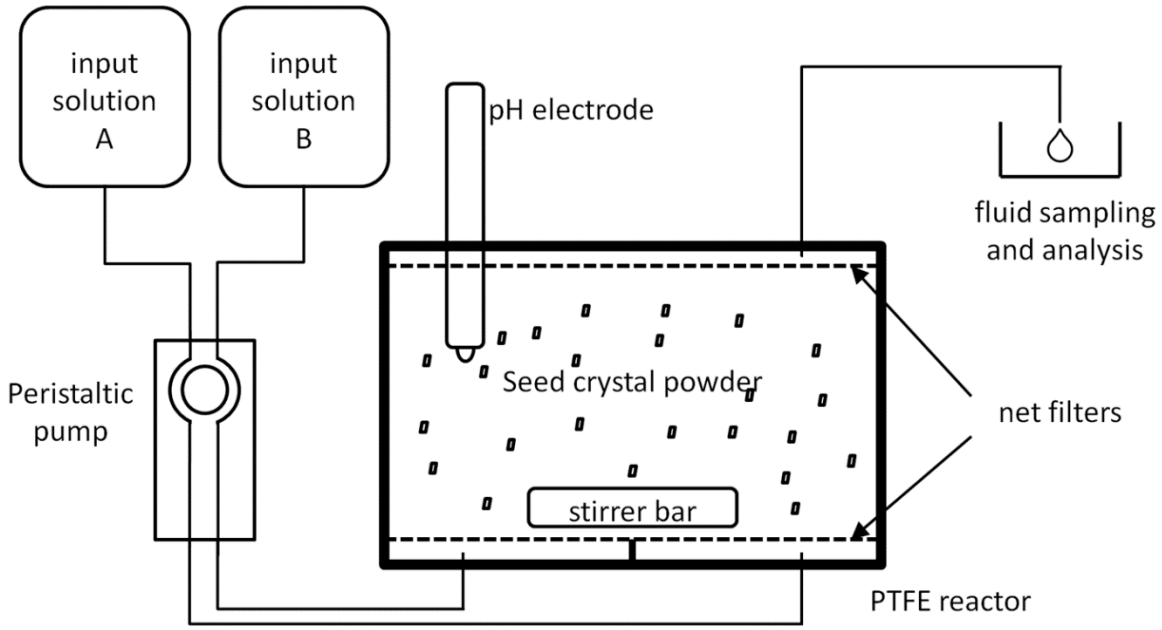

This is a preprint, the final version is subject to change, of the American Mineralogist (MSA)
Cite as Authors (Year) Title. American Mineralogist, in press.
DOI: http://dx.doi.org/10.2138/am-2018-6232

Figure 3

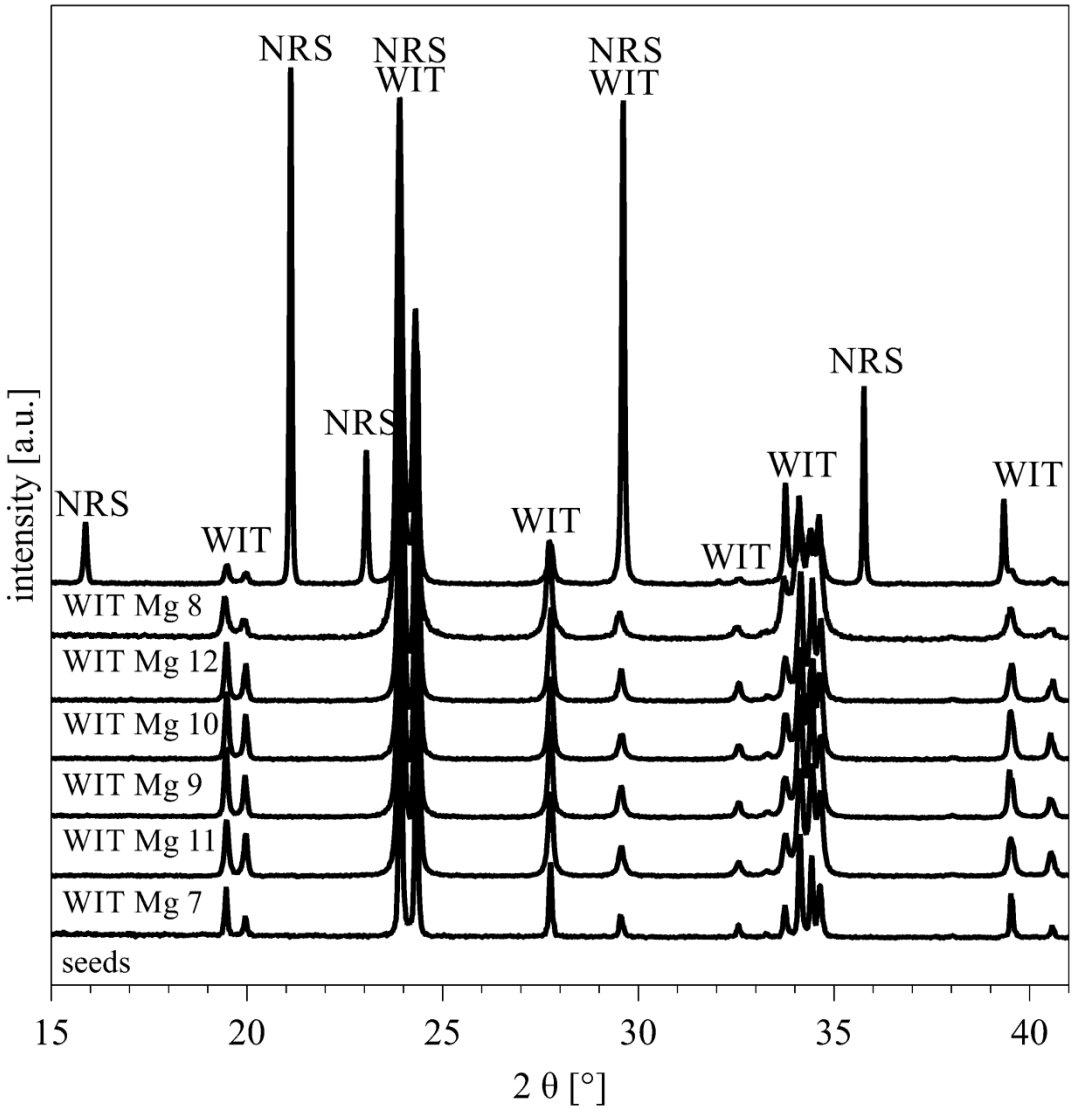

This is a preprint, the final version is subject to change, of the American Mineralogist (MSA)
Cite as Authors (Year) Title. American Mineralogist, in press.
DOI: http://dx.doi.org/10.2138/am-2018-6232

Figure 4

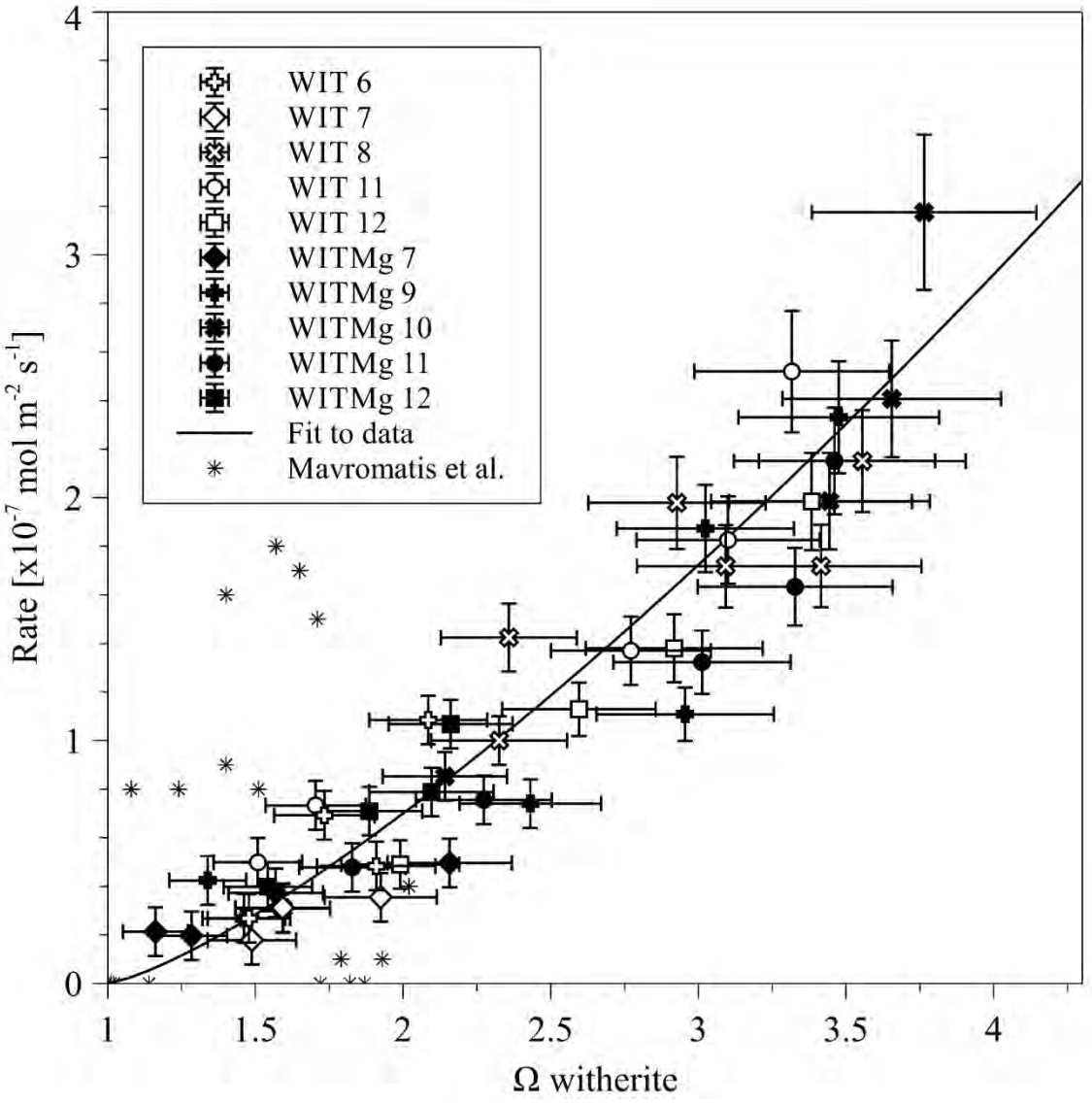

This is a preprint, the final version is subject to change, of the American Mineralogist (MSA)
Cite as Authors (Year) Title. American Mineralogist, in press.
DOI: http://dx.doi.org/10.2138/am-2018-6232

Figure 5